

INVESTIGATING THERMAL BRIDGING IN WINDOW SYSTEMS INSULATED WITH MONOLITHIC SILICA AEROGEL

By

Fariz Dhalla, P.Eng.

Bachelor of Mechanical Engineering

A MRP presented
to Ryerson University
in partial fulfilment for the degree of
Master of Building Science
in the program of
Building Science

Toronto, Ontario, Canada, 2015

© (Fariz Dhalla) 2015

AUTHOR'S DECLARATION FOR ELECTRONIC SUBMISSION OF A MRP

I hereby declare that I am the sole author of this MRP. This is a true copy of the MRP, including any required final revisions.

I authorize Ryerson University to lend this MRP to other institutions or individuals for the purpose of scholarly research.

I further authorize Ryerson University to reproduce this MRP by photocopy or by other means, in total or in part, at the request of other institutions or individuals for the purpose of scholarly research.

I understand that my MRP may be made electronically available to the public.

Abstract

INVESTIGATING THERMAL BRIDGING IN WINDOW SYSTEMS INSULATED WITH MONOLITHIC SILICA AEROGEL

By

Fariz Dhalla, P.Eng.

Master of Building Science, 2015

in the program of Building Science at Ryerson University.

Windows typically account for 30% to 50% of heat losses through building envelopes. Monolithic silica aerogel has thermal properties and physical characteristics which make it an attractive material for high performance glazing. Optimizing the thermal performance of individual window components can improve the thermal performance of windows insulated with monolithic silica aerogel. It is important to consider how the thermal properties can be sustained, especially when in contact with other window components such as edge and intermediate spacers and the window frame.

The purpose of this research paper is to analyze French style windows insulated with four panes of monolithic silica aerogel and investigate the thermal bridging of edge and intermediate spacers and window frame in order to assess how they collectively affect the centre of glass and edge of glass regions. The research aims to determine the spacer geometry, materials, and window frame that guarantee the best performing window system.

Acknowledgments

This research paper would not have been completed without the assistance and expertise of my supervisor Professor Umberto Berardi. I would like to express my sincere gratitude for his contribution and the direction given during the process and successful completion of this research paper.

I would also like to thank Professor Ramakrishnan Ramani for his input on the methodology of this research paper and the audio visual team in the Architectural Science department for their technical support.

Finally, I would like to thank my family, friends, and colleagues for their continuous support and motivation throughout the MRP process.

Dedication

I would like to dedicate this research paper to my mother Nilufa Dhalla. Along with having faith and standing by my decisions, she has taught me to be patient and to quietly work hard, allowing the results to speak for themselves.

Table of Contents

1	Introduction	1
2	Background Research.....	3
2.1	Aerogel	3
2.1.1	Synthesis of Monolithic Aerogel	4
2.1.2	Thermal Conductivity of Aerogel	5
2.1.3	Light and Solar Transmissibility of Aerogel	7
2.1.4	Influence of Aerogel Insulated Windows on Space Heating.....	10
2.1.5	Structural Characteristics of Aerogel	12
2.2	Window Frame.....	12
2.2.1	Solid Wood and Thermally Broken Wooden Window Frame	13
2.2.2	Thermally Broken Window Frame	14
2.3	Edge Sealing	19
2.3.1	Edge Seal Components.....	19
2.3.2	Thermal performance of Edges Seals	21
2.3.3	Window Spacer and Edge Seal Considerations for Aerogel Windows.....	24
3	Scope of Research and Methodology	28
3.1	Development of 3D Model in SolidWorks and COMSOL Multiphysics	29
4	Results.....	38
4.1	Effective Conductivity	38
4.2	U-Value of Window Systems.....	41
4.3	Centre of Glass, Edge of Glass, and Window Frame Segments	49
4.4	Thermographic Heat Transfer Diagram	51
5	Discussion and Conclusion	60
	Appendix 1 – Thermographic Heat Transfer Diagrams.....	63

Appendix 2 – Photographs of Prototype 75
References 76

List of Tables

Table 1 – Conductivity of various insulating materials (Taoning, 2014)	7
Table 2 – Effects of antireflective coatings and low iron glass on solar energy transmittance.....	10
Table 3 – Energy consumption of a single family in a Danish climate (Schultz, 2008)	11
Table 4 - Material properties of window components	30
Table 5 - Simulation model Identification part a	34
Table 6 - Simulation model Identification part b	35
Table 7 - Heat flux (W/m^2) for window systems computed by COMSOL	43
Table 8 – Comparing performance of aerogel insulated window with air filled double glazed window ...	46
Table 9 – U-value (W/m^2k) comparison of results between 1D and 3D analysis	47
Table 10 - Heat flux (W/m^2) and U-value (W/m^2k) for frameless glazing computed by COMSOL	48
Table 11 - Summary of results (U-value, and glazing segment proportions.....	61

List of Figures

Figure 1 - Granular aerogel	3
Figure 2 - Monolithic aerogel.....	3
Figure 3 – Comparing conduction through aerogel with a solid insulating material	6
Figure 4 – Light transmissibility of monolithic silica aerogel (Berardi, 2015)	7
Figure 5 – Characteristics of various glazing systems (Buratti, 2011).....	8
Figure 6 – Prototype of aerogel glazed unit (Schultz, 2008).....	11
Figure 7 – Traditional French style casement window (Berardi, 2015)	12
Figure 8 – Segments of glazing unit (Van Den Bergh, 2012).....	13
Figure 9 – Solid wood window frame	14
Figure 10 – Thermally broken wooden window frame.....	14
Figure 11– Section of generic air cavity (Asdrubali, 2013).....	15
Figure 12 – Section of thermally broken aluminum window frame (Asdrubali, 2013)	17
Figure 13 - Thermal resistance for a series of cavities with high emissive surface treatment.....	18
Figure 14 - Thermal resistance for a series of cavities with low emissive surface treatment.....	18
Figure 15 – Typical methodology for edge seal of insulated glazing unit (Van Den Bergh, 2012)	19
Figure 16 – Cross section of edge seal detail (Van Den Bergh, 2012).....	20
Figure 17 – Edge seal and spacer configuration system (Van Den Bergh, 2012).....	21
Figure 18 – Effects of edge seal system on glass surface temperature (Van Den Bergh, 2012)	22
Figure 19 – Total U-value of spacer system as a function of λ_{eff} (Van Den Bergh, 2012)	23
Figure 20 – Window frame R-value of various spacer system combinations.....	24
Figure 21 - Total glazing U-value as a function of window size with foil rim seal solution	25
Figure 22 - Proposed rim seal detail of aerogel glazed Unit (Schultz, 2005)	26
Figure 23 - Improved rim seal detail of aerogel glazed unit with polystyrene edge (Schultz, 2005)	26
Figure 24 – Schematic of window showing elements analyzed	29
Figure 25 – Edge and intermediate spacer details (modelled using SolidWorks)	31
Figure 26 – Window frame details (modelled using SolidWorks).....	32
Figure 27 – Boundary conditions for heat transfer analysis in COMSOL.....	37
Figure 28 – Effective conductivity of window frames (λ_{eff}).....	39
Figure 29 – Effective conductivity of spacers (λ_{eff}).....	40
Figure 30 – Performance of Window Systems (3D Analysis)	41

Figure 31 – Performance of Window Systems (3D Analysis)	44
Figure 32 – Illustration of frameless glazing	48
Figure 33 – Centre of glass, edge of glass, and window frame segment percentages	50
Figure 34 – Thermographic heat transfer diagram (Solid Wood Window)	52
Figure 35 – Thermographic heat transfer diagram (Thermally Broken Wooden Window).....	54
Figure 36 – Thermographic heat transfer diagram (Thermally Broken Aluminum Window).....	56
Figure 37 – Thermographic heat transfer diagram (Vinyl Window)	58

1 Introduction

Windows are irreplaceable features in buildings because they introduce daylight, fresh air, and provide an outdoor view for building occupants. However, from a thermal point of view, windows are often a weak point having a larger U-value compared to other building envelope components. Many previous studies have investigated the energy performance of windows. Currently the most popular commercial windows are double glazed, balancing both performance and cost. Windows insulated with monolithic silica aerogel are a type of high performance window which may enhance the thermal performance of building enclosures. Monolithic silica aerogel has favourable thermal properties and physical characteristics with enhanced visible transmissibility compared to the granular form. The highly porous lightweight material has a thermal conductivity less than still air. However, the fragile nature of the material limits the maximum crack free size to 580mm x 580mm (Shultz, 2005), suggesting that they are better suited for French style windows.

Optimizing the thermal performance of individual window components can improve the thermal performance of windows insulated with monolithic silica aerogel. Studies indicate that insulated spacers meet structural requirements, while have better thermal performance, compared to conventional metal spacers. Low conductive materials with thin profiles can minimize thermal bridging around the perimeter of the window. Studies have shown that edge spacers with effective conductivities less than 2W/mK can reduce the edge of glass region, inherently increasing the performance of a glazing unit (Asdrubali, 2013).

This research paper focuses on investigating thermal bridging of edge and intermediate spacers and window frame forming French style windows insulated with monolithic silica aerogel. The 0.5mm thick edge and intermediate spacer profiles studied include 'U', 'H', 'X', and 'T' and the materials assessed include aluminum, stainless steel, and PVC. Solid wood and thermally broken wood, aluminum, and vinyl window frames along with the spacers were analyzed together to determine which window system guarantee the best performing window with monolithic silica aerogel. Solid Works was used to produce 3D models of each window system and a finite element heat transfer analysis was undertaken using COMSOL Multiphysics, to determine the overall heat flux, effective conductivities, and thermographic heat transfer diagrams of each window system, simulated with winter conditions. Finally, results from

the 3D analysis were compared against a fundamental 1D analysis to show variations and to demonstrate the advantage of a 3D heat transfer analysis.

2 Background Research

2.1 Aerogel

Aerogel is a material that has existed for over 80 years. It is a highly porous dried gel material which was first developed by Dr. Samuel Kistler in the 1930s. Aerogel is lightweight and is derived from gel where the liquid component of the gel is replaced with a gas. When the liquid is removed, the result is a highly porous, low density, and puffy looking solid material.

There are two types of aerogels which could be used for high performance windows: granular and monolithic. Granular aerogel as shown on Fig. 1, consists of small translucent grains of gel material compacted together and would typically be placed between panes of glass. Monolithic aerogel as shown on Fig. 2 is a solid transparent tile of gel material which could also be placed between panes of glass. As aerogel is a low density material with over 90% porosity, it becomes difficult to handle larger sized tiles due to its fragility. There are size limitations for monolithic aerogel tiles when compared to granular aerogels, which are more favourable for larger glazing units. However, monolithic aerogel have better thermal properties and better solar energy transmittance compared to the granular form, making it a material of interest especially for glazing units in heating dominated regions of the world. Granular aerogels are used today in windows, whereas monolithic aerogels are not as established.

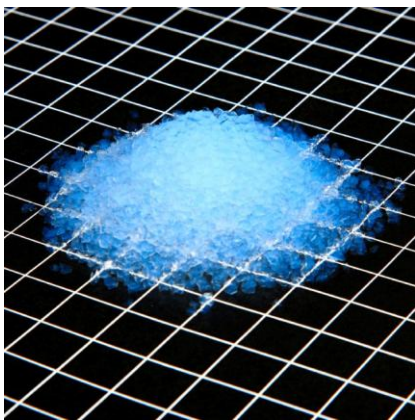


Figure 1 - Granular aerogel

(Source: <http://www.aerogel.org>)



Figure 2 - Monolithic aerogel

(Source: <http://www.aerogel.org>)

2.1.1 Synthesis of Monolithic Aerogel

The synthesis of silica aerogel involves three steps:

1. Gel Preparation
2. Aging
3. Drying

Gel preparation or sol gel process is a process in which solid nanoparticles dispersed in a liquid solution agglomerate together to form a continuous three dimensional network throughout the liquid eventually reaching what is known as the gel point (Baetens, 2010). Important characteristics of the sol gel process such as growth rate, degree of cross-linking, and colloid size are controlled by factors such as polarity of the solvent, ionic strength of the reaction medium, and temperature. The mechanical rigidity of the gel is enhanced by the degree of cross linking of the nanoparticles (Shukla, 2014).

The purpose of the aging process is to provide sufficient time for strengthening the silica network. This is achieved by controlling the pH level, concentration of particles, and water content of the covering solution. After the aging process, all of the water must be removed before the supercritical drying process. This is accomplished by washing the gel with ethanol and heptanes. Remaining moisture would yield an opaque and very dense looking aerogel material.

Drying of the gel is the final and most critical step in the production process of aerogel. There are two methods of drying: ambient pressure drying and supercritical drying. Ambient pressure drying causes shrinkage and possible fracture because of small pores and resulting capillary tension. In order to produce an effective aerogel material, the preferred drying process is supercritical drying where liquid within the pores is removed while above its critical temperature and pressure, avoiding capillary tension. Liquid within the pores must be replaced with air. If a liquid is held under a pressure greater than its vapour pressure and the temperature is raised, the liquid will transform into a gas without two phases being present at a given time (Baetens, 2010).

Low temperature supercritical drying with carbon dioxide is the method used to produce aerogel materials for building applications. Aged gel is placed in an autoclave that is filled with non-flammable

liquid carbon dioxide at a temperature between 4⁰C to 10⁰C, at a pressure of 100bar (Baetens, 2010). The vessel is slowly heated above the solvent critical temperature and pressure (i.e. $T_{cr} = 304.2^0\text{K}$, $P_{cr} = 72.786\text{atm}$) (Baetens, 2010). When all the solvents are replaced, the autoclave is heated to 313⁰K while maintaining a pressure of 100bar. The fluid is then slowly depressurized. Finally, the autoclave is cooled to room temperature at ambient pressure. If the drying process is carried out correctly, the result is a highly porous transparent monolithic aerogel material with a density ranging from 70kg/m³ to 270kg/m³ (Fricke, 1987).

2.1.2 Thermal Conductivity of Aerogel

High performance windows with U-values below 1W/m²k can be constructed in several ways. The most common approach is a triple glazed system using low emissivity coatings and noble gas filling of gaps between the transparent glass layers. The benefit of increasing the number of glass panes in a window is a higher thermal resistance with an inherent reduced U-value. However, the drawback for increasing the number of glass panes is a low transmission of solar energy and reduced daylight transmission, both of which would have a negative impact on the total energy balance of the window, especially in heating dominated climates (Duer, 1998). Finally, increasing the quantity of glass would require a wider window frame, increase the overall weight of the window assembly, and drive up production costs.

A monolithic aerogel pane placed in the air layer between glass panes could reduce the convection heat loss between the panes of glass without compromising daylight and solar transmittance (Buratti, 2011) Monolithic aerogel is a highly porous material with pore sizes ranging from approximately 10nm to 100nm (Schultz, 2005). The porosity is generally above 90% making it a highly insulating material with a thermal conductivity lower than still air (<0.025W/mK). Aerogel has a thermal conductivity between 0.015W/mK to 0.02W/mK under atmospheric pressure (Duer, 1998).

Monolithic aerogel is made up of small three dimensional intertwined clusters which comprise of approximately 3% of the volume (Aspen, 2014). As aerogel has a high porosity, the contact surface area between the clusters is much smaller compared to the surface area of a typical homogenous solid insulating material. Conduction through the aerogel material is much lower compared to the solid insulation material. The inner skeleton structure has many dead ends, resulting in ineffective heat transfer paths (Berardi, 2015). Figure 3 demonstrates how aerogel achieves a lower heat loss by conduction when compared to a typical solid insulating material.

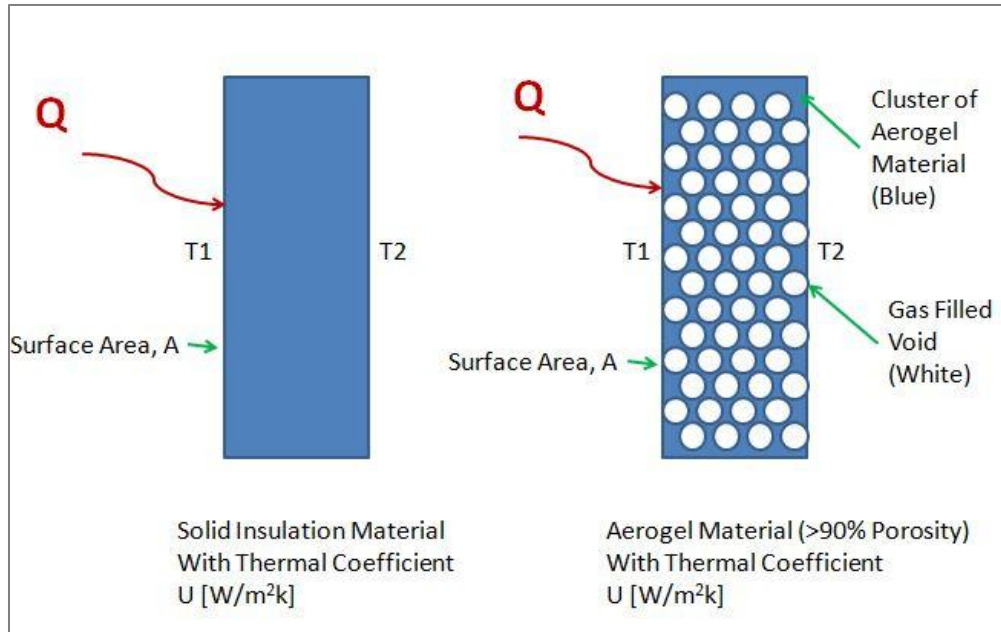


Figure 3 – Comparing conduction through aerogel with a solid insulating material

The remaining 97% of volume in monolithic aerogel is comprised of air within nanopores. The air within the nanopores has very little room to move, inhibiting both convection and gas phased conduction. Thus, the heat transfers through the material mainly by conduction and radiation within the solid skeleton structure. The skeleton structure, made up of 90% air voids, limits conduction. At a partial vacuum with a pressure less than 5000Pa, the thermal conductivity could be further reduced to below 0.01W/mK (Duer, 1998). The thermal resistance of a 20mm evacuated aerogel tile would provide the same thermal resistance of 100mm conventional mineral wool insulation (Duer, 1998). Table 1 compares the conductivity of various insulating materials.

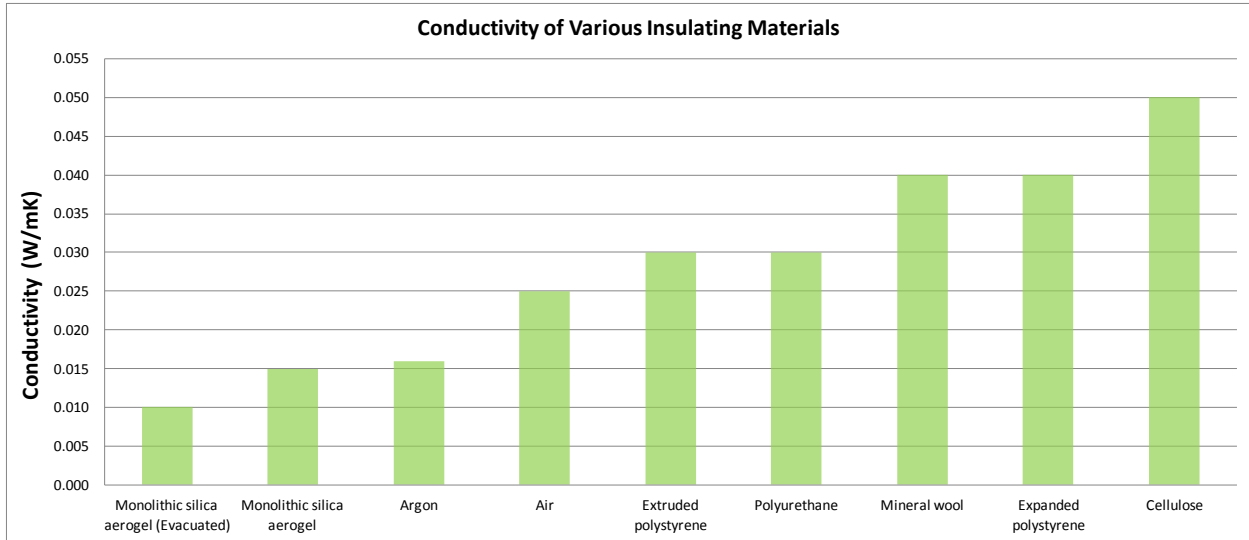


Table 1 – Conductivity of various insulating materials (Taoning, 2014)

2.1.3 Light and Solar Transmissibility of Aerogel

Figure 4 shows the average light transmittance of three samples. The dashed line describes the relationship of a monolithic aerogel panel, the solid grey line describes the relationship of an air filled glazing unit, and the solid black line describes the relationship of a monolithic aerogel panel sandwiched between two glass panes.

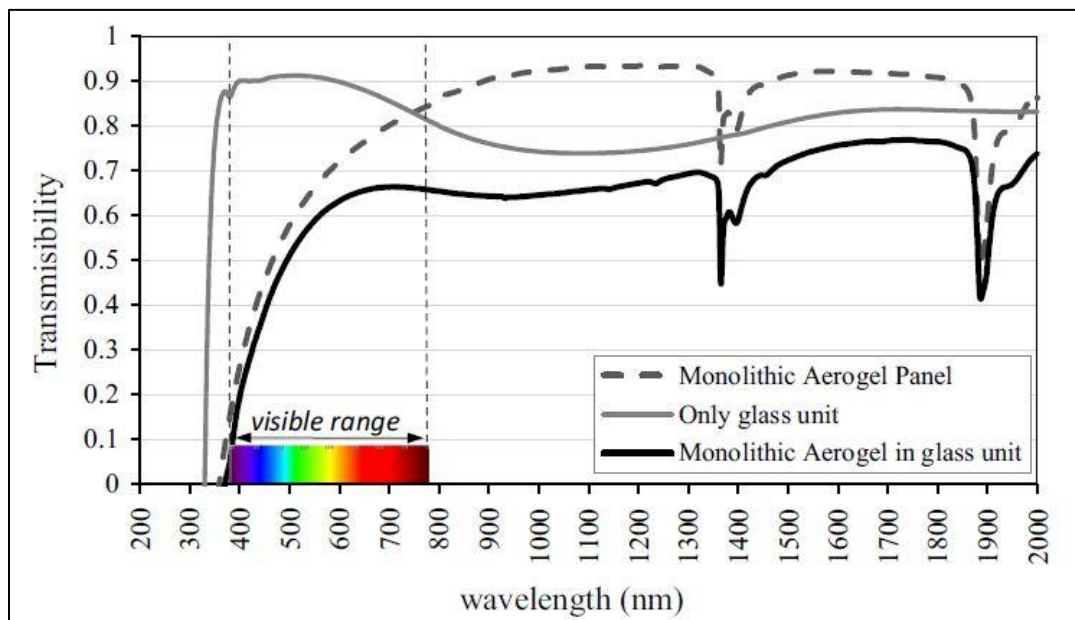


Figure 4 – Light transmissibility of monolithic silica aerogel (Berardi, 2015)

Comparing results with the glass unit, monolithic aerogel transmits less light at shorter wavelengths, within the visible spectrum, which is between 390nm and 700nm. However, the opposite holds true at longer wavelengths ($850\text{nm} < \lambda < 1350\text{nm}$ and $1400\text{nm} < \lambda < 1850\text{nm}$) where the transmissibility increases before dropping again. The transmissibility plot of the monolithic aerogel panel sandwiched between panes of glass follows the profile of the monolithic aerogel panel but the light transmissibility is generally less than the glass unit. This is because properties of the glass allow it to reflect and absorb light, while at certain longer wavelengths; the aerogel also tends to absorb light, affecting the overall light transmissibility of the monolithic aerogel glass unit.

Figure 5 compares the performance of various glazing systems characterized by the same 4mm pane of float glass on the interior and exterior with various intermediate layers. The figure compares the visible transmissibility (TV), solar transmissibility (g), and U-value (U) for various glazing systems. As noted on Fig. 5, a conventional window is defined as a double glazed window with 4mm panes of float glass, 12mm intermediate air gap, and a 4mm low e coating (Burrati, 2011).

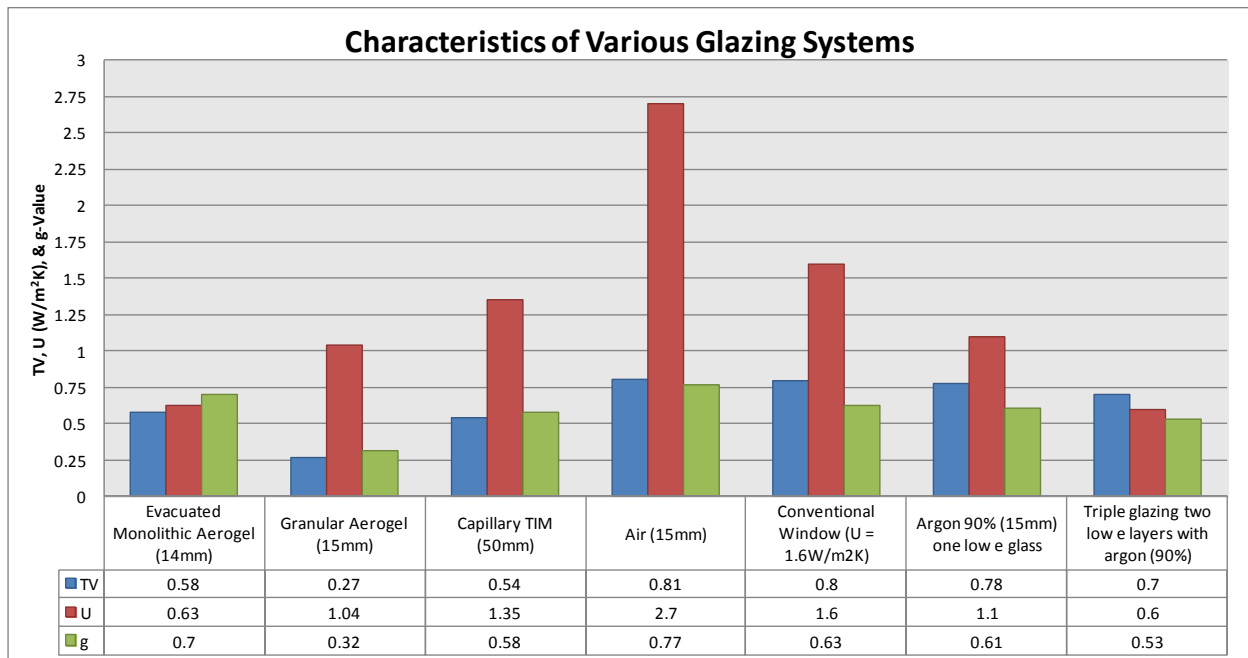


Figure 5 – Characteristics of various glazing systems (Buratti, 2011)

The results on Fig. 5 indicate that developed aerogel glazing units have a total solar energy transmittance higher than a conventional window and at the same time have approximately the same

heat loss coefficient of a triple glazed gas filled glazing unit. The above results also indicate that the visible transmittance of an aerogel glazing system is approximately 27% less compared to the conventional window. This is because of the scattering and diffusive properties of aerogel materials. In theory, the small pore sizes make it possible to produce a perfectly transparent silica aerogel. However, during the production process, local disorders in the material result in scattering of transmitted light mainly in the blue part of the visible spectrum. The scattering of light gives a hazy look when observed through aerogel but also changes colours in such a way that aerogel appears slightly bluish in a dark background and a slightly yellowish in lighter background (Duer, 1998). The scattering of light is most visible when the aerogel is exposed to direct sunlight.

Monolithic silica aerogel has a higher solar transmittance compared to the granular form. A 10mm thick monolithic aerogel window can have a solar transmittance of up to 0.9, whereas a granular silica aerogel window can have a maximum solar transmittance of approximately 0.5 (Berardi, 2015). Monolithic aerogel is the only known material that has a good combination of high solar and light transmittance and low thermal conductivity. These characteristics make it possible to achieve a net energy gain during heating season for north facing windows in Europe or south facing windows in Canada. The utilization of the passive solar energy passing through a window is an important factor in reducing the annual energy consumption for space heating. This was the background for the HILIT research and development projects (Shultz, 2005). The objective for this project was to improve the aerogel elaboration process with respect to thermal and optical properties, improve the manufacturing process, and finally to develop a glazing unit with a U-value lower than 0.6W/mK with a total solar energy transmittance exceeding 75%.

Again, the advantage of aerogel glazing compared to other highly insulated glazing units is the high solar energy transmittance value (g-value), which in cold climates has a large influence on the annual energy consumption. The basic 15mm thick monolithic silica aerogel developed as part of the HILIT project had a solar transmittance of 70%. It was found that after a subsequent heat treatment process at a temperature of 425°C, the solar energy transmittance increased to 76% (Schultz, 2005). However, when placing aerogel between two planes, the solar transmittance is reduced due to absorptive and reflective properties of the adjacent glass panes. A common 4mm pane of float glass absorbs about 10% of the solar radiation while the iron content tends to change the colour of the transmitted daylight. It was concluded that float glass with low iron content could reduce the solar absorption to less than 1%,

independent of the glass thickness (Schultz, 2005). The reflection losses of glass panes amount to about 8%. SUNARC A/S, a Danish company, has developed a surface treatment which reduces reflection losses to approximately 3% (Schultz, 2005). In summary, the calculated solar energy transmittance of a monolithic aerogel glazing unit sandwiched between low iron content float glass, treated with SUNARC's surface treatment was estimated to be 82% (Schultz, 2005). Table 2 compares the total solar energy transmittance for aerogel glazing and commercial low energy glazing with antireflective treated low iron glass. All glazing units have a heat loss coefficient of approximately $0.6\text{W/m}^2\text{kK}$ and all the glass panes have a thickness of 4mm while the aerogel pane has a thickness of 15mm.

Solar Energy Transmittance		
Glazing type	Common float glass (%)	Anti reflective treated low iron glass (%)
Triple glazed unit	45	59
Aerogel glazed unit	67	82

Table 2 – Effects of antireflective coatings and low iron glass on solar energy transmittance

(Schultz, 2005)

The above figure demonstrates the benefits of using antireflective coated low iron glass for both aerogel and low energy glazing units. There is an improvement of approximately 15% for both types of glazing. It is interesting to notice that a low energy glazing unit, with low iron glass, treated with antireflective coatings, yields a solar energy transmittance lower than an aerogel unit, which is not optimized with low iron glass and antireflective coatings. An optimized triple glazed unit has solar energy transmittance of 59% while the solar energy transmittance of an aerogel unit without being optimized has a solar energy transmittance of 67%.

2.1.4 Influence of Aerogel Insulated Windows on Space Heating

An analysis was performed on a single family home in a Danish climate. The analysis assumed an aerogel glazing system with a U-value of $0.5\text{W/m}^2\text{K}$ and a total solar energy transmittance of 0.75. The thickness of monolithic aerogel used was 20mm. The energy consumption was compared with a triple glazed argon filled glazed unit with a U-value of $0.6\text{W/m}^2\text{K}$ and solar transmittance of 0.46. Table 3 compares the calculated annual energy demand for space heating for two houses insulated according to the Danish building code and to the passive house standards installed with either triple glazed argon filled glazing or with an evacuated aerogel glazed unit.

Building insulation level	Space heating demand (kWh/year)	
	Triple glazing	Aerogel glazing
Building code	6220	5040
Passive house	2070	1380

Table 3 – Energy consumption of a single family in a Danish climate (Schultz, 2008)

Table 2 indicate that the energy demand is reduced by 19% for a house with evacuated aerogel glazing built to the Danish building code (Schultz, 2008). The energy demand for a house built to passive house standards is reduced by approximately 34% (Schultz, 2008). Figure 6 is a prototype of an evacuated aerogel glazed unit.



Figure 6 – Prototype of aerogel glazed unit (Schultz, 2008)

Although aerogel glazed units are promising during heating season, measures should be taken to prevent overheating during warmer summer months. This will reduce the cooling load, inherently reducing the energy demand.

2.1.5 Structural Characteristics of Aerogel

Aerogel is very vulnerable to tensile stress and also to moisture. The material must be effectively protected from the environment if used for ordinary building applications, especially as an insulating material for windows. Aerogel is however very strong in compression. It is a material suitable for sandwich construction and can be inserted between panes of glass (Duer, 1998). Due to the fragility of monolithic aerogel, there are size limitations for handling and production purposes. The largest crack free monolithic aerogel slab developed for HILIT project measured 580mm x 580mm with a thickness of 15mm. Further reinforcement and a larger autoclave for supercritical drying would be required to develop larger sized aerogel tiles. Monolithic aerogel could be better suited for retrofitting traditional French casement type windows as shown on Fig. 7. Smaller and structurally stable tiles could be produced and installed at each section.

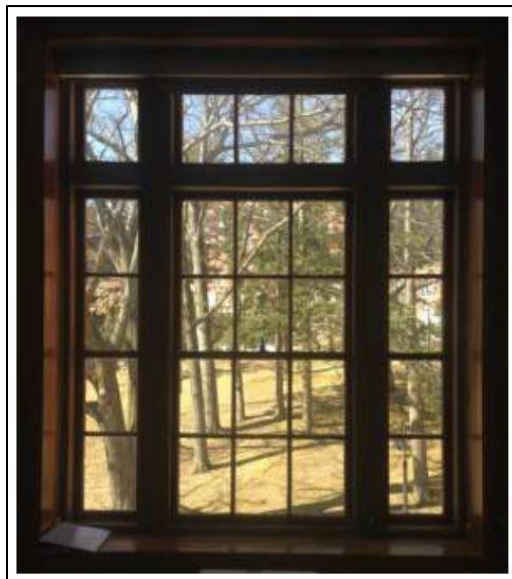


Figure 7 – Traditional French style casement window (Berardi, 2015)

2.2 Window Frame

The thermal performance of a window is important for energy efficient buildings. Although today's state of the art windows have considerably lower U-values compared to windows of the past, the heat loss per area through windows is much greater compared to the opaque walls and roof of a building. Windows typically account for about 30-50% of the transmission losses through the building envelope, regardless of the window wall ratio (Gustavsen, 2011). Walls and roof of a building can easily achieve U-

values ranging from $0.1\text{W/m}^2\text{k}$ to $0.2\text{W/m}^2\text{k}$. U-value for windows typically vary between $0.8\text{W/m}^2\text{k}$ to $2.4\text{W/m}^2\text{K}$, whereas commercial double glazed windows with low e coating and argon filling have a thermal transmittance of $1.1\text{W/m}^2\text{k}$ (Van Den Bossche, 2015). However, the best windows have a U-value ranging from $0.6\text{W/m}^2\text{k}$ to $0.8\text{W/m}^2\text{k}$ (Gustavsen, 2011). Translucent aerogel insulated windows have a U-value ranging from $0.3\text{W/m}^2\text{k}$ to $0.5\text{W/m}^2\text{k}$. Figure 8 shows how a glazing unit can be broken down into the following segments: window frame, edge of glass region, and centre of glass region.

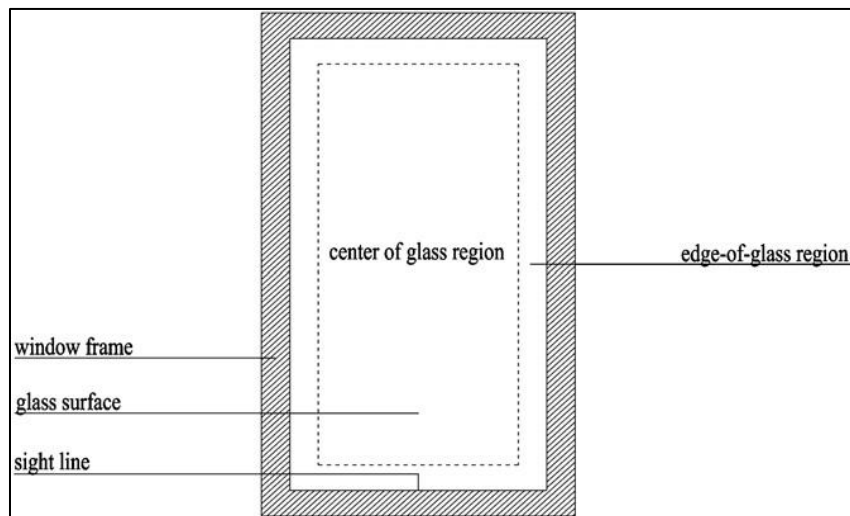


Figure 8 – Segments of glazing unit (Van Den Bergh, 2012)

The edge of glass region is described as the perimeter of glass between the edge of the frame and the point where the glass surface temperature is the same as the temperature at the centre of glass. The edge of glass band can range from 63mm to 102mm (Van Den Bergh, 2012). Low temperature in this region increases the potential for condensation, leading to mold growth, deterioration of window frames, window seals, and wall sections in cold climates. A key energy strategy for window frames is to use low conductivity materials and components, which would minimize the edge of glass band and the thermal transmittance through a window, decreasing heat loss from the warm interior space to the colder exterior during winter months, and vice versa during summer months. Therefore the design of each single component of a window becomes an important task.

2.2.1 Solid Wood and Thermally Broken Wooden Window Frame

Aluminum window frames are typically chosen based on their cost effectiveness, durability, and their minimal maintenance requirements. Wooden window frames however; have the potential to have a

much lower thermal transmittance. Softwoods such as Cedar, Fir, Pine, and Spruce are better insulators compared to hardwoods such as Ash, Birch, Maple, and Oak. However, softwoods are less durable and more susceptible to premature deterioration but if shielded accordingly from the environment, softwoods are still preferred (Van Den Bergh, 2015). Thermal performance of solid wood frames can be improved by inserting a thermal break of polyurethane foam, in the middle section of the frame. Figures 9 and 10 show the cross sections of a typical solid wood and thermally broken wooden window frames respectively.

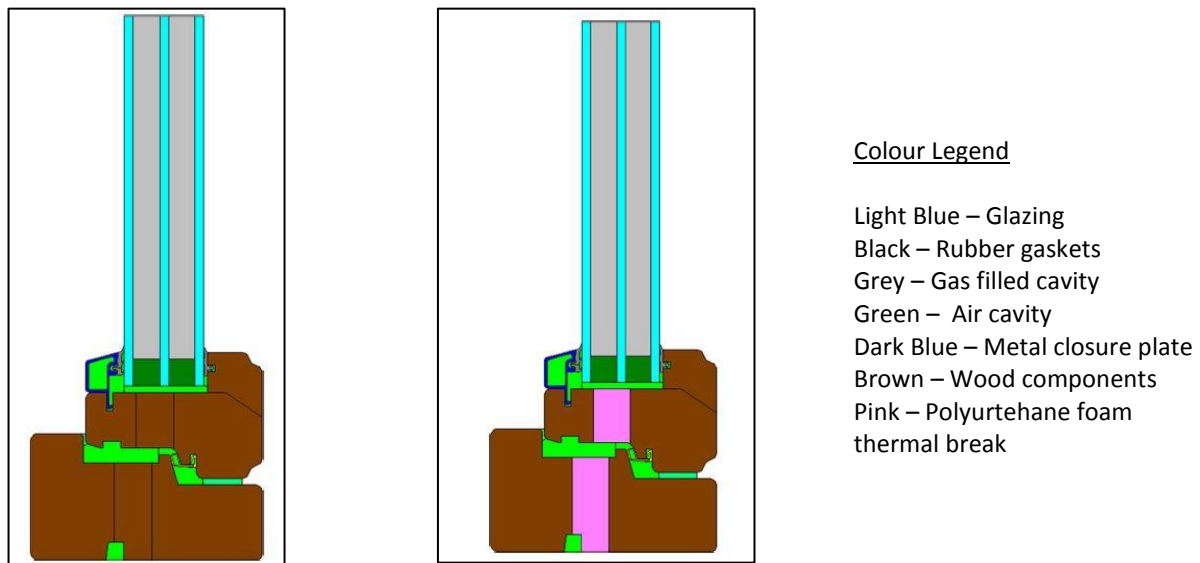


Figure 9 – Solid wood window frame
(Gustavsen, 2011)

Figure 10 – Thermally broken wooden window frame
(Gustavsen, 2011)

2.2.2 Thermally Broken Window Frame

The purpose of a thermally broken window frame is to reduce heat loss by direct conduction. Particular attention is given to metal frames which have a high thermal conductivity. The performance of a metal frame can be improved by using thermal breaks and by introducing unvented air cavities (Asdrubali, 2013). The mode of heat transfer within the air cavities is a result of natural convection and radiation. Several factors affect the thermal transmission through thermally broken frames, which include geometry of the cavity, its position, and emissivity of solid surfaces. Thermophysical properties of the gas including its thermal conductivity, specific heat capacity, thermal expansion coefficient, and dynamic

viscosity also affect the thermal transmission. The air cavity is typically treated as a solid component with an associated equivalent conductivity. Figure 11 is a generic section of an air cavity, where (b) is the width of the cavity, (d) is the depth of the cavity, (q) is the heat flux, and (ϵ_1) and (ϵ_2) is the emissivity of surface 1 and 2 respectively.

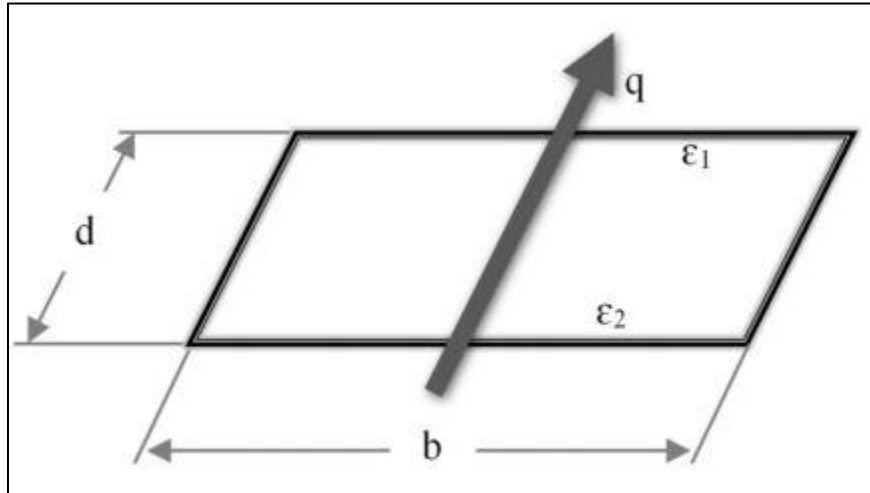


Figure 11– Section of generic air cavity (Asdrubali, 2013)

The equivalent conductivity is therefore expressed with the following relationship, where R_s is the thermal resistance of the cavity in m^2K/W .

$$\lambda_{eq} = d/R_s \quad [1]$$

$$R_s = 1/ (h_a + h_r) \quad [2]$$

The heat transfer occurring by conduction and convection inside the cavity can be described by the following relationship, where C_1 and C_2 are constants for evaluating convection coefficients, and have values of $0.025W/mK$ and $0.73W/m^2k^{4/3}$ respectively (Asdrubali, 2013).

$$h_a = \max \{C_1/d; C_2\Delta T^{1/3}\} \quad [3]$$

The maximum is chosen between a value which depends on the cavity depth (d) or resistance by conduction, and another value which is proportional to the temperature difference between the inner and outer surfaces or resistance by convection (Asdrubali, 2013).

The heat transmission by radiation inside the cavity can be described by the following relationship

$$h_r = 4\sigma T_m^3 EF \quad [4]$$

Where,

σ is the Stefan Boltzmann constant and it is equal to $5.67 \times 10^{-8} \text{ W/m}^2\text{k}^4$;

T_m is the average temperature in the cavity;

F is the view factor for a rectangular section and,

E is the emittance between surface 1 and 2.

Thermal transmission by radiation is influenced by the emissivity of the cavity's inner surfaces. One low emissive surface is enough to substantially reduce the heat transfer inside the cavity. Most cavities have high emissive surfaces because of painted components. It is essential to determine the emissivity of each metal surface treatment to assess the heat transfer through a window frame profile.

Window frames are typically designed with numerous air cavities confined by aluminum components or by gaskets, forming thermal breaks. Figure 12 shows a section of a thermally broken aluminum window frame with unvented air cavities.

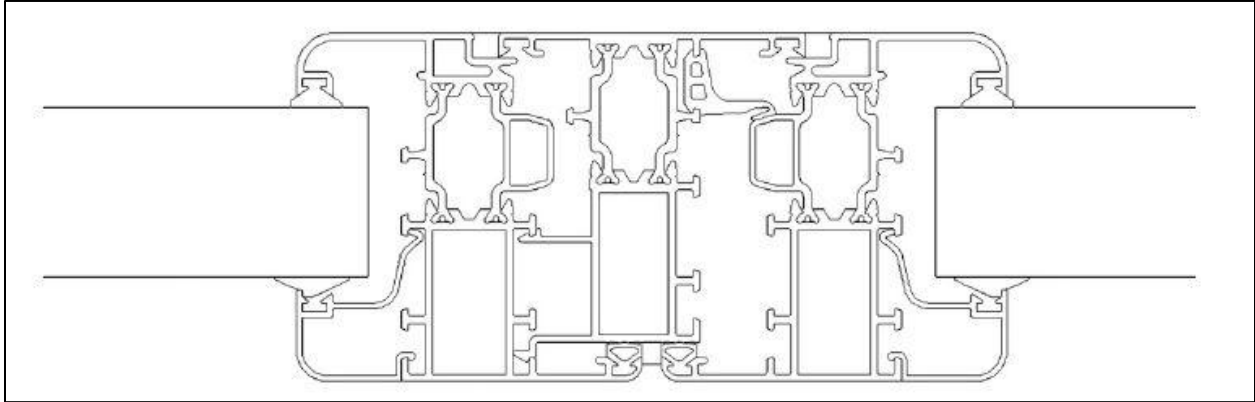


Figure 12 – Section of thermally broken aluminum window frame (Asdrubali, 2013)

Gaskets are used to minimize conduction heat transfer through metal components and to divide cavities, reducing depth and, consequently reducing the equivalent conductivity of the window frame. In order to simulate a typical profile for a window frame, a cavity of a total depth could be subdivided into a variable number of cavities. The temperature on the extreme surfaces of the profile would be constant while the temperatures of the faces of the single gaps are changed proportionally to the total number of cavities. The optimal depth is equal to 20mm, assuring high thermal performance with reasonable sized air gaps (Asdrubali, 2013).

Figures 13 and 14 show the convection and radiation heat transmission coefficients and the total resistance as a function of the number of cavities for cavities with high emissive and low emissive surfaces respectively. In summary when evaluating the combined influence of convection and radiation heat transmission, the total resistance varies significantly with surface treatment. The thermal resistance of high emissive cavities is dependent on the radiation coefficient. Low emissive cavities increase the total resistance of the network of cavities, and variation of total resistance depends on the convection coefficient, where cavity depth and temperature difference between surfaces become critical variables.

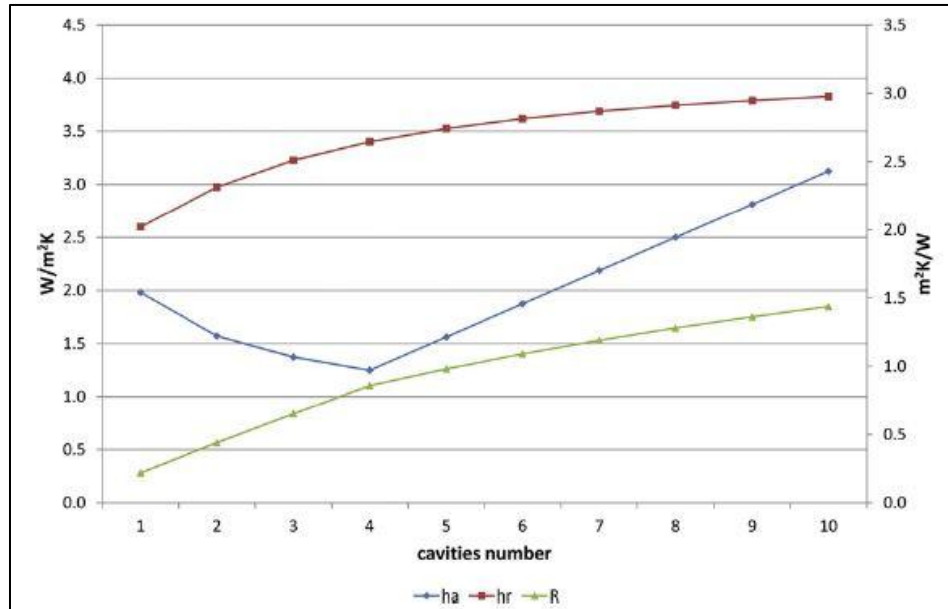


Figure 13 - Thermal resistance for a series of cavities with high emissive surface treatment (Asdrubali, 2013)

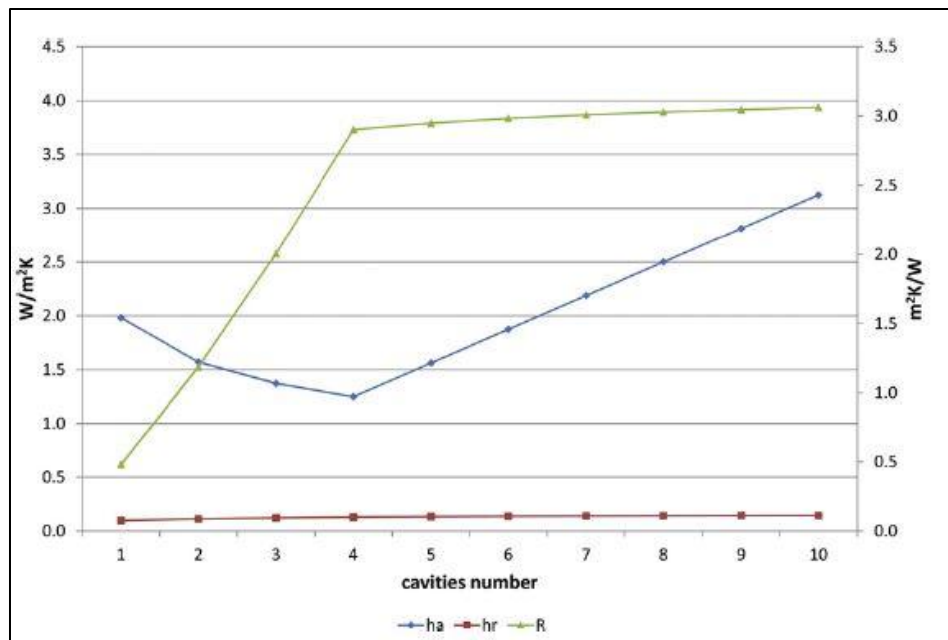


Figure 14 - Thermal resistance for a series of cavities with low emissive surface treatment (Asdrubali, 2013)

2.3 Edge Sealing

Insulated glazing units consist of multiple glass panes that are structurally held together along the perimeter by various types of edge seal systems. A key function of edge seals is to maintain and keep the glass panes separated at equal distance, while providing moisture and air tightness. Figure 15 shows the typical geometry of an edge seal for an insulated glazing unit.

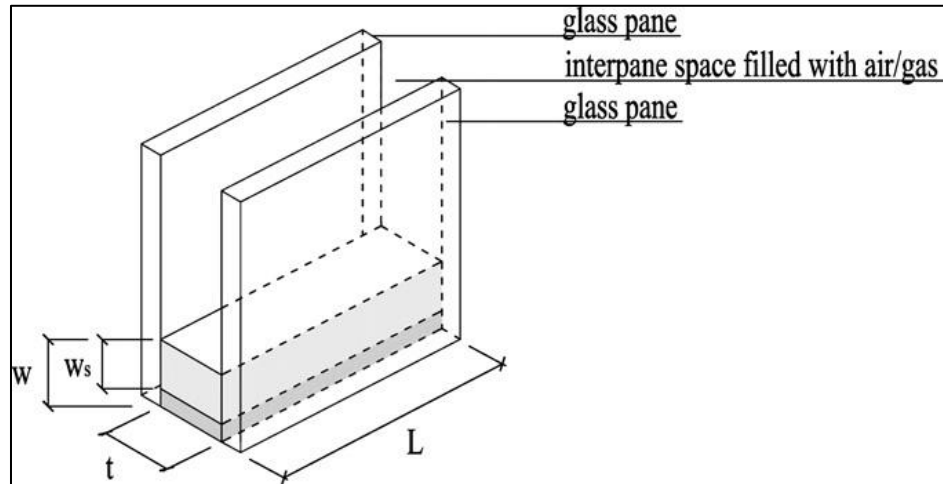


Figure 15 – Typical methodology for edge seal of insulated glazing unit (Van Den Bergh, 2012)

The width (W) of an edge seal typically ranges from 8mm to 12mm, while the thickness (t) typically depends on factors such as number of glass panes, type of gas fill, and acoustical requirements. Most commercial windows have thicknesses ranging from 6mm to 24mm.

2.3.1 Edge Seal Components

The edge seal consists of a spacer bar, desiccant, and a sealant. Figure 16 shows the cross section of a single sealed (left) and double sealed (right) insulated glazing unit.

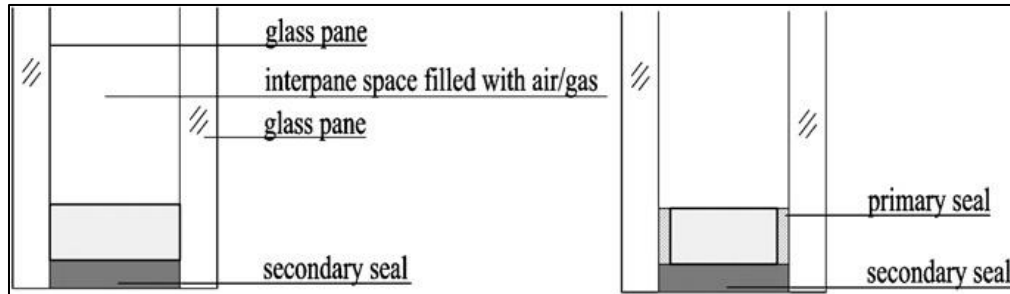


Figure 16 – Cross section of edge seal detail (Van Den Bergh, 2012)

Spacer bars provide spacing of glass panes at a fixed distance. The width (W_s) of commercial spacer bars is typically between 4mm to 8mm. Spacer bars must be mechanically stable and provide tightly sealed corner connections, which are achieved by metal or plastic corner keys or more commonly by bent spacer corners.

Sealants structurally bond glass panes and spacer bars together, while providing air and moisture tightness. Sealants also have a certain flexion characteristic to accommodate deflection from the glass. Majority of the insulating glazing units are dual sealed. Synthetic rubbers such as polyisobutylene are used as a primary sealer and are applied between the spacer and the glass panes. They are typically 0.2mm to 0.6mm thick and their function is to reduce moisture and gas permeability into the edge of glass region of the glazing unit. The strength of thermoplastics such as polyisobutylene decreases as temperature increase. Also, the seal's adhesion to the glass and spacer is not resistant to continuous water exposure. A secondary sealer is required to guarantee the structural integrity of a glazing unit. The 4mm adhesive secondary sealer unites the glass panes and spacer bar, preventing movement under fluctuating environmental conditions and mechanical stresses. The best secondary sealant available today has a conductivity of about 0.24W/mK (Van Den Bergh, 2012). However, good adhesion and durability are more important requirements for a secondary sealant, which may limit thermal improvements that are realistically possible.

Desiccants are used to prevent fogging between panes of glass because of condensation from moisture and organic vapours. Moisture can get trapped inside the interpane area during the manufacturing process. Chemical fogging occurs when organics react with glass surfaces within the interpane area, leaving a permanent opaque deposit on the inside of the glass surface. Desiccants can prolong a window's service life by adsorbing moisture and organic vapour until it is saturated. They can be

integrated in edges seals or used as a fill in hollow perforated spacer bars. Relative humidity and pores sizes affect the adsorption capabilities of desiccant materials.

2.3.2 Thermal performance of Edges Seals

Spacer bars for glazing units were traditionally made of aluminum or galvanized steel. The thermal conductivity of metal spacers increases thermal bridging at the edge of glass region. Edge seals have a significant influence on the overall U-value of a glazing system. The use of insulated spacer bars and thermally improved edge seals can considerably reduce heat loss through a glazing unit. Figure 17 shows 10 edge seal and spacer configuration systems.

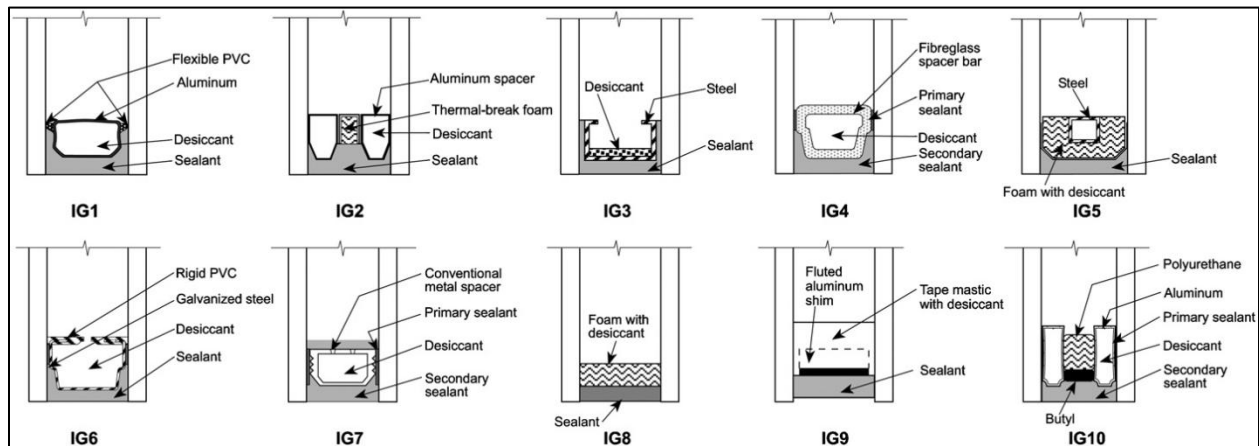


Figure 17 – Edge seal and spacer configuration system (Van Den Bergh, 2012)

Numerical investigations show that a windows total U-value is reduced by 6% when traditional spacer replaced with an insulating spacer in a standard double glazed wood framed window (Van Den Bergh, 2012). Triple glazed units or glazing systems with low emissivity coatings can reduce total U-value by 12% if insulated spacers are used over traditional aluminum spacers (Van Den Bergh, 2012). Figure 18 shows the effects of the various edge seal techniques shown on Fig. 17 above on the glass surface temperature (warm side).

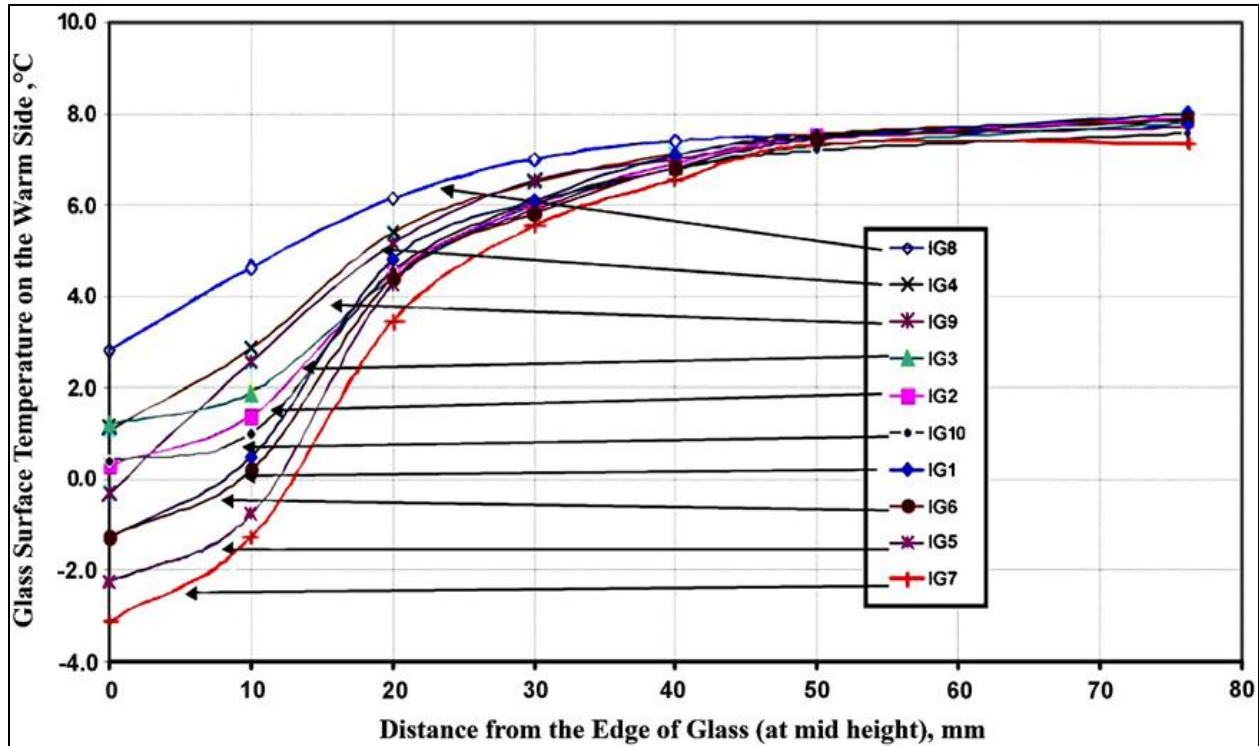


Figure 18 – Effects of edge seal system on glass surface temperature (Van Den Bergh, 2012)

Insulated spacer bars lead to higher glass surface temperatures on the edge of glass region compared to temperatures experienced when conventional metal spacers are used, inherently lowering the U-value of a glazing unit.

Studies have shown that a frame and edge of glass U-value decrease with decreasing spacer conductivity. Changing the effective spacer conductivity from 10W/mK to 0.25W/mK, decreases frame U-value by 18% to 36%, depending on frames thermal properties (Van Den Bergh, 2012). The effective spacer conductivity is found by converting the real spacer assembly into a simple homogenous solid. The conductivity of the solid block is equal to the effective conductivity of the real spacer assembly. Spacers containing aluminum or stainless steel have an effective conductivity between 2W/mK to 10W/mK and 0.3W/mK to 1W/mK respectively. Insulated spacers have an effective conductivity between 0.2W/mK to 0.3W/mK. Pure materials used as spacers such as aluminum, stainless steel, and insulating elements have thermal conductivities of 160W/mK, 17W/mK, and approximately 0.2W/mK respectively (Gustavsen, 2011). The effective conductivity of a spacer system cannot be directly compared to the conductivity of a pure material.

Studies have found a logarithmic relationship between the overall U-value of a spacer system and its effective conductivity (Van Den Bergh, 2012). Figure 19 shows that the total spacer system U-value curve flattens out for spacer systems with an effective conductivity greater than 2 W/mK.

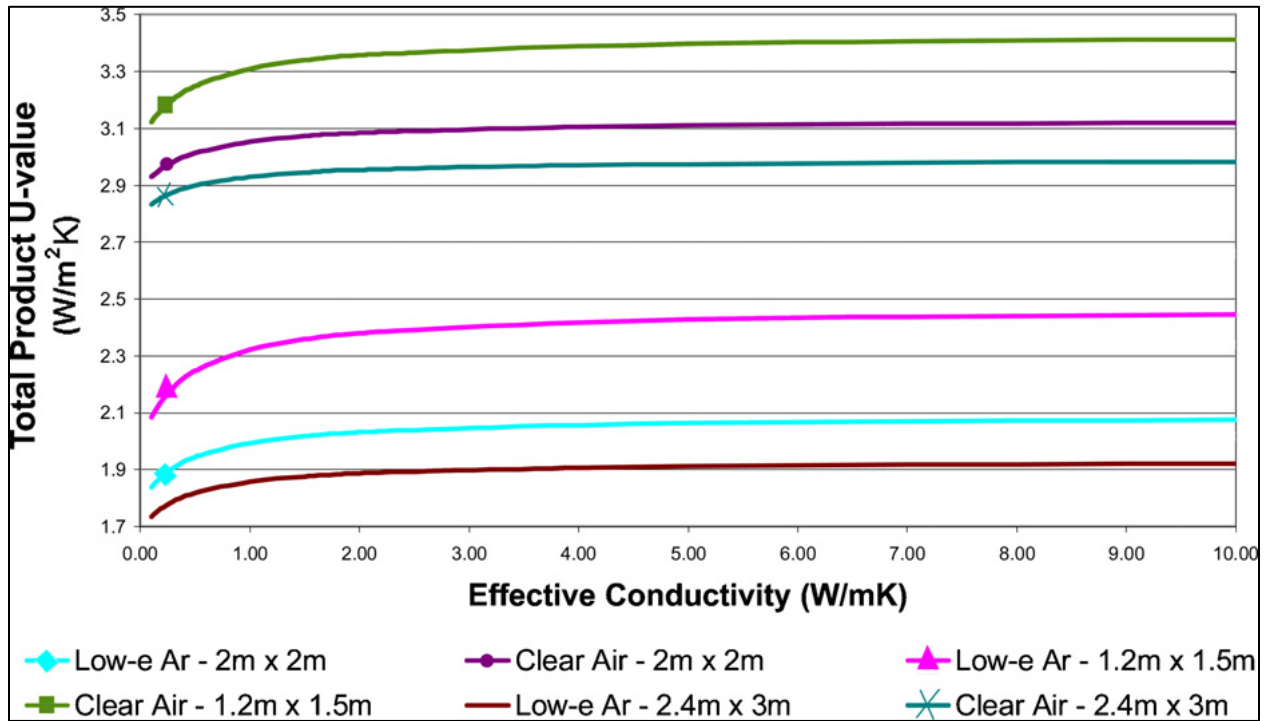


Figure 19 – Total U-value of spacer system as a function of λ_{eff} (Van Den Bergh, 2012)

Studies have been done to see how the 10 spacer systems shown on Fig. 17 affect the overall resistance of window frames under laboratory conditions. The 10 spacers were placed between two clear 1.0m x 1.0m panes of glass, with air in the glazing cavity. Vinyl, thermally broken aluminum, solid redwood, and foam filled fibreglass were the four window frame materials tested. Figure 20 compares the thermal resistance of various window systems.

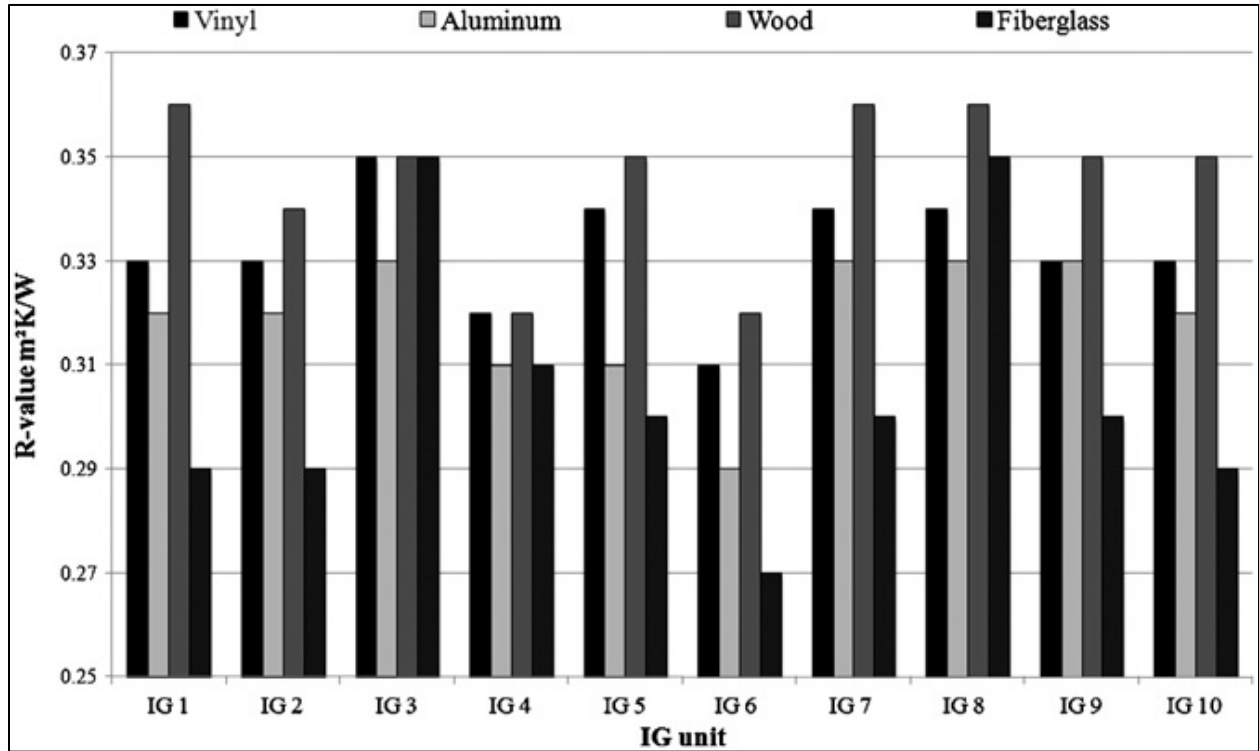


Figure 20 – Window frame R-value of various spacer system combinations (Van Den Bergh, 2012)

Although wood frames performed better, the results cannot be necessarily generalized. In this case, relative performance is more important than the absolute resistance value because of differences in design, detailing, and manufacturing processes of the window frames that were tested (Van Den Bergh, 2012).

2.3.3 Window Spacer and Edge Seal Considerations for Aerogel Windows

Using materials with low thermal conductivity, minimizing material thickness, and increasing the heat flow path are effective ways to minimize thermal bridging (Schultz, 2005). An ideal rim seal should provide sufficient gas and moisture tightness while structurally maintain the desired spacing between the glass panes. In an aerogel glazing unit, the aerogel pane would have sufficient strength to serve as a spacer between the panes of glass. The rim seal for an aerogel glazing unit does not necessarily need structural strength, but more serve as a gas and vapour barrier. Glass is considered too fragile and the only suitable options for rim sealing materials are metal and laminated plastic foils. Metal foils less than 0.1mm are not airtight due to pinholes. However, metal foils with a thickness greater than 0.1mm tend

to be 100% tight against gas and moisture diffusion. Laminated plastic foils developed for vacuum insulated panels also have a very low permeability and could be a sufficient material for a limited lifetime. The Mylar 250 RSBL developed by DuPont is made up of several different plastic layers and a 13nm thick aluminum layer. With an overall thickness of 0.1mm, the Mylar plastic foil is sufficient to maintain a 100% seal for at least 30 years if protected against water and UV radiation (Schultz, 2005). Figure 21 shows the relationship between U-value as a function of window size with various foil rim seal solutions. Line (a) is a plot for a window which has a 0.2mm stainless steel rim seal, line (b) is a plot for a 0.1mm stainless steel rim seal, line (c) is a plot for a 0.05mm stainless steel rim seal, and line (d) is a plot for the Mylar 250 RSBL300 laminated plastic seal typically used in vacuum insulated panels.

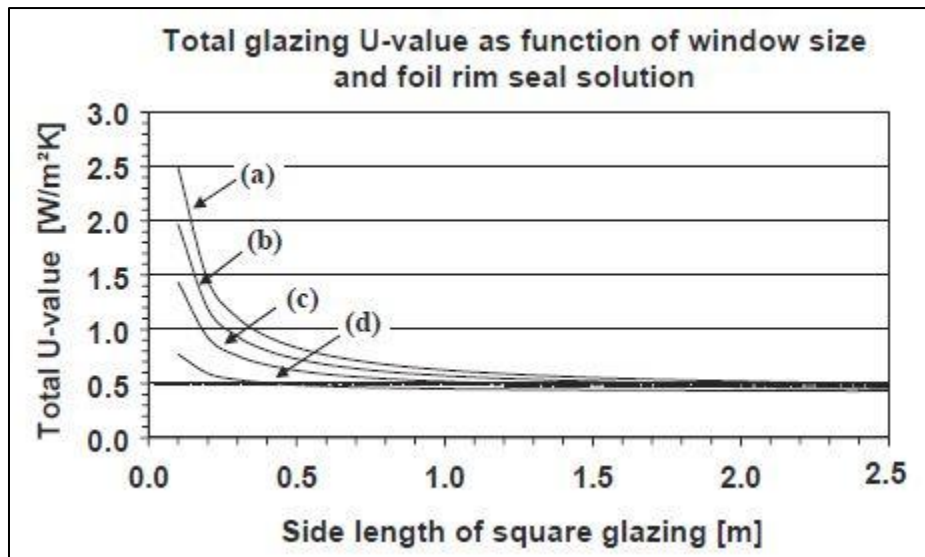


Figure 21 - Total glazing U-value as a function of window size with foil rim seal solution (Schultz, 2005)

The results of the plot on Fig. 21 demonstrate that as the size of the aerogel glazed window increases, the effects of thermal bridging at the rim seal is reduced. The plot also demonstrates that using materials with lower conductivity and with a small thickness can also reduce the effects of thermal bridging at the rim seal. Figure 22 describes the typical assembly process for applying and rim seal of an aerogel glazed unit.

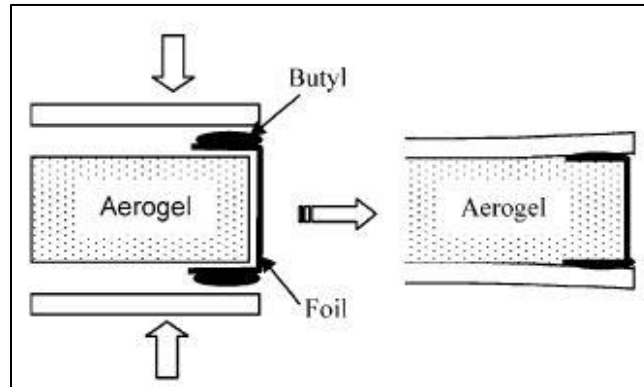


Figure 22 - Proposed rim seal detail of aerogel glazed Unit (Schultz, 2005)

The assembly process above is referred as the self tightening principal for evacuated aerogel glazed units. This is because during evacuation, the atmospheric pressure presses the glass panes against the aerogel while the butyl sealant makes a firm airtight joint between the foil and the glass panes. Furthermore, the permeability of both foil and butyl sealant is very low and leads to a theoretical lifetime of 100 years for a completely perfect seal. However, temperature fluctuations lead to thermal stresses to both the glazing and butyl sealant which combined with aging would reduce the glazing lifetime. The lifespan is estimated to be between 20 to 25 years (Schultz, 2005).

The drawback to the above assembly technique is that the glazing unit will not be flat around the perimeter. The bending of the glass pane would result in tensile stresses at the glass edges requiring the use of tempered glass to avoid breakage. Furthermore, careful care must be taken while wrapping foil around the edges of the aerogel as it is a fragile material to handle. Figure 23 shows an improved rim seal detail.

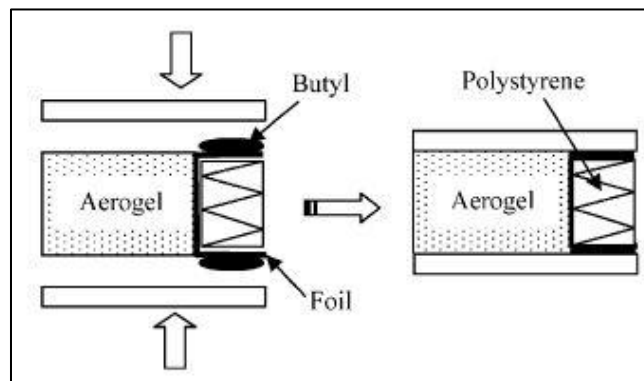


Figure 23 - Improved rim seal detail of aerogel glazed unit with polystyrene edge (Schultz, 2005)

The HILIT project developed a detail where the foil is folded around a polystyrene spacer. The height of the polystyrene spacer would be a few millimeters lower than the thickness of the aerogel, accommodating space for the butyl seal. With this rim seal technique, a flat glazed unit is achieved while handling the foil and application of the butyl sealant can be done without touching the aerogel edges. However, the thicker edge seal would increase the thermal bridging effects and the likelihood of air leakages around the glazing unit.

3 Scope of Research and Methodology

Findings from the background research were the guidelines for investigating the thermal bridging in window systems insulated with monolithic silica aerogel. The purpose of the research was to determine the spacer geometry, materials, and window frame that guarantee the best performing window with monolithic silica aerogel.

The research methodology was undertaken with the following steps:

1. 3D models of window systems including the edge and intermediate spacers and window frames were modelled using SolidWorks. The foundation for designing the window systems was developed from the background research, which focused on properties of monolithic silica aerogel, window frames, and edge spacers;
2. The SolidWorks models were imported into COMSOL Multiphysics where a 3D finite element heat transfer analysis was undertaken with defined boundary conditions;
3. The total heat flux of the window systems, effective conductivities of the spacers and window frames, and thermographic heat transfer diagrams were produced using COMSOL;
4. A 1D heat transfer analysis was performed where the area weighted U-value was calculated for each modelled window system;
5. Using the heat flux found from the 3D heat transfer simulation in COMSOL, a U-value was determined and compared with the 1D analysis and,
6. Thermographic heat transfer diagrams were used to demonstrate the proportion of edge of glass, centre of glass, and window frame regions of the modelled window systems.

3.1 Development of 3D Model in SolidWorks and COMSOL Multiphysics

A number of applications were used to investigate the thermal bridging in window systems insulated with monolithic silica aerogel. SolidWorks, a 3D CAD tool was used to produce 3D models of each window system.

There are size limitations for monolithic silica aerogel because of their fragile properties. The maximum crack free aerogel pane produced in the HILIT project measured 580mm x 580mm (Shultz, 2005). A French style window was modelled in SolidWorks consisting of 4 quadrants. The size of the 6mm inner and outer glass panes excluding the frame was 1040mm x 1040mm, while each aerogel quadrant was 499mm x 499mm. There is a perimeter edge spacer and intermediate edge spacers dividing the window into quadrants. Figure 24 is a schematic of a window system showing the various elements that were analyzed, and photographs of the prototypes constructed may be seen on Appendix 2.

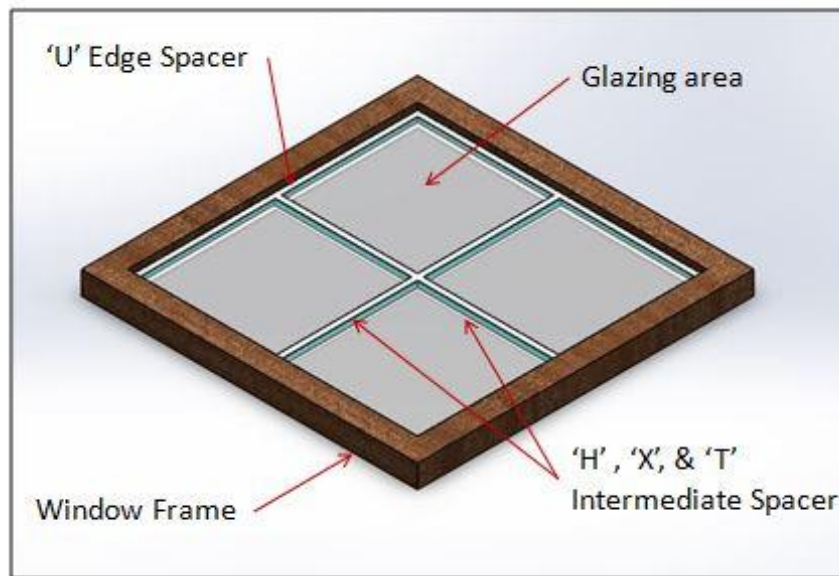


Figure 24 – Schematic of window showing elements analyzed

The SolidWorks models were imported into COMSOL Multiphysics, where a 3D finite element heat transfer analysis was undertaken. The heat transfer module in COMSOL uses material conductivity (k), density (ρ), and specific heat capacity (c_p) for analyzing conduction through solid and fluid materials. The material properties assigned to the various window components for simulating heat transfer through the window systems are outlined on Table 4.

Material	k [W/mK]	ρ [kg/m ³]	cp [J/kgK]
Aluminum	160	2800	880
Stainless Steel	14.9	7900	477
XPS Foam Insulation	0.027	55	1210
Plastic (PVC)	0.19	1400	1050
Wood (hardwood)	0.16	720	1255
Wood (softwood)	0.12	510	1380
Float Glass	1	2500	750
Polysulfide	0.4	1700	1000
Aerogel	0.015	100	2100
Air	0.025	1.225	1000
Polyamide	0.25	1150	1600
Rubber	0.13	1100	2010

Table 4 - Material properties of window components

The material and geometry of edge and intermediate spacers was analyzed to determine which variable reduces the edge of glass region, inherently improving the performance of the window system. The spacer materials which were analyzed include aluminum, stainless steel, and polyvinyl chloride (PVC). A 'U' profile insulated spacer bonded with a polysulfide secondary seal was used as the edge spacer forming the perimeter of the glazing unit. The intermediate spacer profiles were 'H', 'X', and 'T'. The purpose of the intermediate spacer is to maintain distance between the glass panes, while also securing adjacent aerogel panes. The logic behind selecting the geometry of the spacers was to lengthen the heat transfer path between the panes of glass. The thickness of all spacers was kept constant at 0.5mm. Figure 25 shows the spacers modelled using SolidWorks.

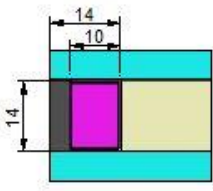
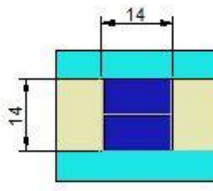
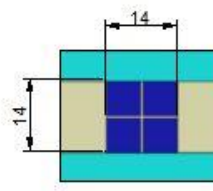
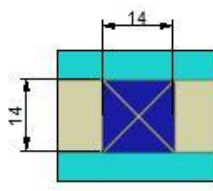
			
<p><u>'U' Edge Spacer</u> Light Blue – Glazing Grey – Polysulfide secondary seal Pink – XPS foam thermal break Black – Edge spacer Beige – Monolithic Silica Aerogel pane</p>	<p><u>'H' Intermediate Spacer</u> Light Blue – Glazing Blue – Unvented air cavity Grey – Intermediate spacer Beige – Monolithic Silica Aerogel pane</p>	<p><u>'T' Intermediate Spacer</u> Light Blue – Glazing Blue – Unvented air cavity Grey – Intermediate spacer Beige – Monolithic Silica Aerogel pane</p>	<p><u>'X' Intermediate Spacer</u> Light Blue – Glazing Blue – Unvented air cavity Grey – Intermediate spacer Beige – Monolithic Silica Aerogel pane</p>

Figure 25 – Edge and intermediate spacer details (modelled using SolidWorks)

Solid wood, thermally broken wood, thermally broken aluminum, and vinyl window frames were also analyzed along with the spacers. Figure 26 shows the cross section of the 4 frames modelled in SolidWorks.

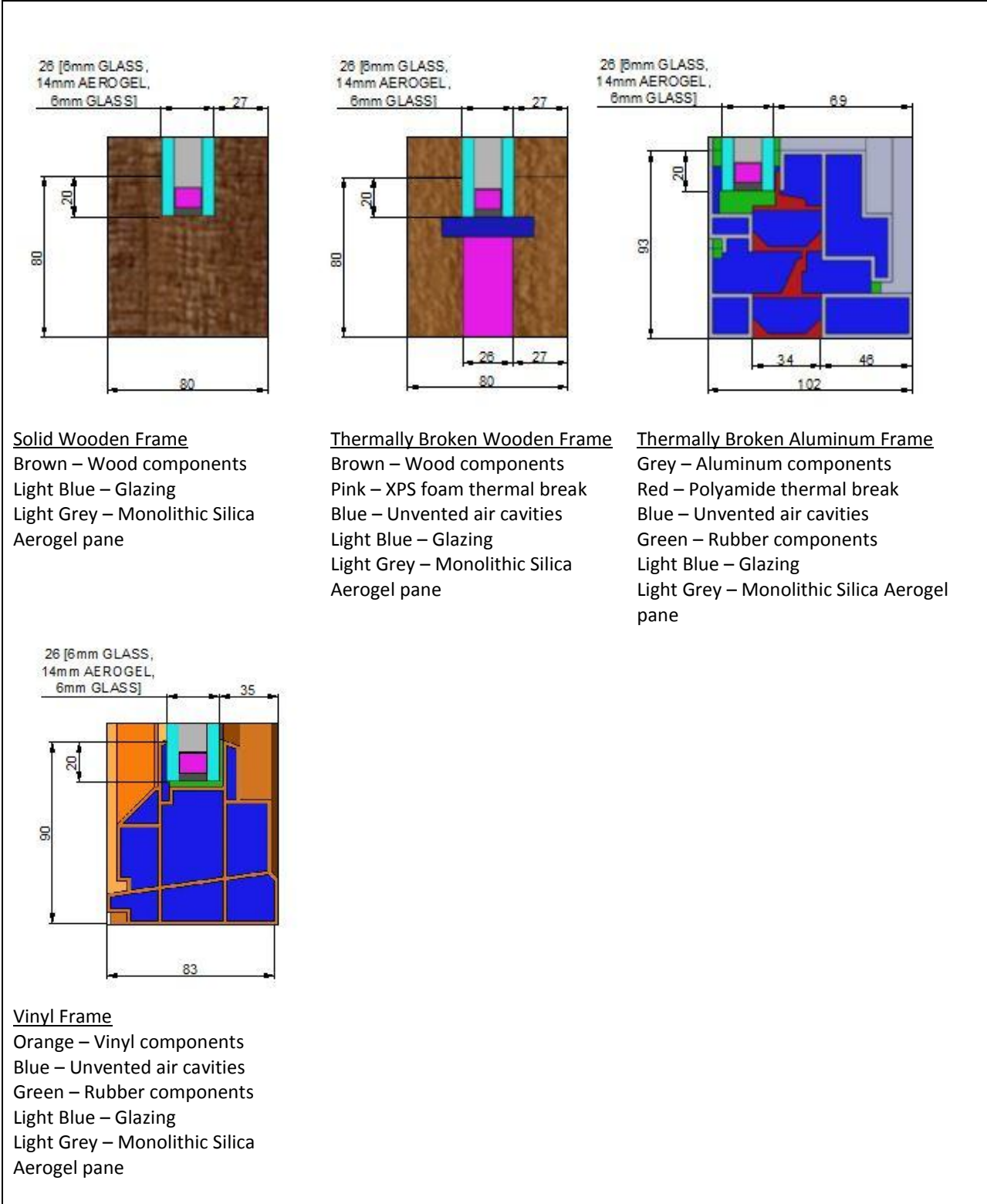


Figure 26 – Window frame details (modelled using SolidWorks)

The French style windows are symmetrical and heat transfer analysis was undertaken on one quadrant to simplify the COMSOL solution. The result of the COMSOL heat transfer analysis was the total heat flux (W/m^2) and subsequently the U-Value ($\text{W}/\text{m}^2\text{K}$) for each window system. The effective conductivity (W/mK) of the edge and intermediate spacers and window frame was also determined using COMSOL. A thermographic heat map of each window system was also produced to demonstrate the proportion of the edge of glass, centre of glass and window frame regions. In total, 36 simulations were performed, and they are coded and described on Tables 5 and 6.

Frame	Model #	Description
Solid Wood Frame	UHWA6146_W_AL	U Edge Spacer, H Intermediate Spacer, 6mm Glass, 14mm Gap (Aerogel), 6mm Glass, Solid Wood Frame, Aluminum Spacer
	UXWA6146_W_AL	U Edge Spacer, X Intermediate Spacer, 6mm Glass, 14mm Gap (Aerogel), 6mm Glass, Solid Wood Frame, Aluminum Spacer
	UTWA6146_W_AL	U Edge Spacer, T Intermediate Spacer, 6mm Glass, 14mm Gap (Aerogel), 6mm Glass, Solid Wood Frame, Aluminum Spacer
	UHWA6146_W_SS	U Edge Spacer, H Intermediate Spacer, 6mm Glass, 14mm Gap (Aerogel), 6mm Glass, Solid Wood Frame, Stainless Steel Spacer
	UXWA6146_W_SS	U Edge Spacer, X Intermediate Spacer, 6mm Glass, 14mm Gap (Aerogel), 6mm Glass, Solid Wood Frame, Stainless Steel Spacer
	UTWA6146_W_SS	U Edge Spacer, T Intermediate Spacer, 6mm Glass, 14mm Gap (Aerogel), 6mm Glass, Solid Wood Frame, Stainless Steel Spacer
	UHWA6146_W_PVC	U Edge Spacer, H Intermediate Spacer, 6mm Glass, 14mm Gap (Aerogel), 6mm Glass, Solid Wood Frame, PVC Spacer
	UXWA6146_W_PVC	U Edge Spacer, X Intermediate Spacer, 6mm Glass, 14mm Gap (Aerogel), 6mm Glass, Solid Wood Frame, PVC Spacer
	UTWA6146_W_PVC	U Edge Spacer, T Intermediate Spacer, 6mm Glass, 14mm Gap (Aerogel), 6mm Glass, Solid Wood Frame, PVC Spacer
Thermally Broken Wood Frame	UHWA6146_TBW_AL	U Edge Spacer, H Intermediate Spacer, 6mm Glass, 14mm Gap (Aerogel), 6mm Glass, Thermally Broken Wooden Frame, Aluminum Spacer
	UXWA6146_TBW_AL	U Edge Spacer, X Intermediate Spacer, 6mm Glass, 14mm Gap (Aerogel), 6mm Glass, Thermally Broken Wooden Frame, Aluminum Spacer
	UTWA6146_TBW_AL	U Edge Spacer, T Intermediate Spacer, 6mm Glass, 14mm Gap (Aerogel), 6mm Glass, Thermally Broken Wooden Frame, Aluminum Spacer
	UHWA6146_TBW_SS	U Edge Spacer, H Intermediate Spacer, 6mm Glass, 14mm Gap (Aerogel), 6mm Glass, Thermally Broken Wooden Frame, Stainless Steel Spacer
	UXWA6146_TBW_SS	U Edge Spacer, X Intermediate Spacer, 6mm Glass, 14mm Gap (Aerogel), 6mm Glass, Thermally Broken Wooden Frame, Stainless Steel Spacer
	UTWA6146_TBW_SS	U Edge Spacer, T Intermediate Spacer, 6mm Glass, 14mm Gap (Aerogel), 6mm Glass, Thermally Broken Wooden Frame, Stainless Steel Spacer
	UHWA6146_TBW_PVC	U Edge Spacer, H Intermediate Spacer, 6mm Glass, 14mm Gap (Aerogel), 6mm Glass, Thermally Broken Wooden Frame, PVC Spacer
	UXWA6146_TBW_PVC	U Edge Spacer, X Intermediate Spacer, 6mm Glass, 14mm Gap (Aerogel), 6mm Glass, Thermally Broken Wooden Frame, PVC Spacer
	UTWA6146_TBW_PVC	U Edge Spacer, T Intermediate Spacer, 6mm Glass, 14mm Gap (Aerogel), 6mm Glass, Thermally Broken Wooden Frame, PVC Spacer

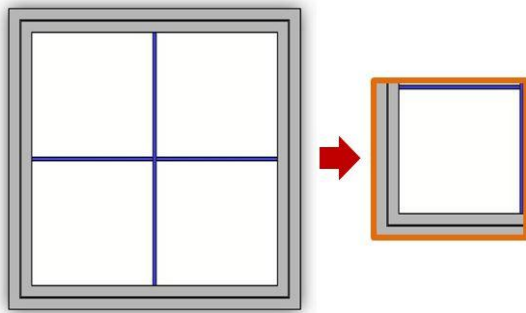
Table 5 - Simulation model Identification part a

Frame	Model #	Description
Thermally Broken Aluminum Frame	UHWA6146_TBAL_AL	U Edge Spacer, H Intermediate Spacer, 6mm Glass, 14mm Gap (Aerogel), 6mm Glass, Thermally Broken Aluminum Frame, Aluminum Spacer
	UXWA6146_TBAL_AL	U Edge Spacer, X Intermediate Spacer, 6mm Glass, 14mm Gap (Aerogel), 6mm Glass, Thermally Broken Aluminum Frame, Aluminum Spacer
	UTWA6146_TBAL_AL	U Edge Spacer, T Intermediate Spacer, 6mm Glass, 14mm Gap (Aerogel), 6mm Glass, Thermally Broken Aluminum Frame, Aluminum Spacer
	UHWA6146_TBAL_SS	U Edge Spacer, H Intermediate Spacer, 6mm Glass, 14mm Gap (Aerogel), 6mm Glass, Thermally Broken Aluminum Frame, Stainless Steel Spacer
	UXWA6146_TBAL_SS	U Edge Spacer, X Intermediate Spacer, 6mm Glass, 14mm Gap (Aerogel), 6mm Glass, Thermally Broken Aluminum Frame, Stainless Steel Spacer
	UTWA6146_TBAL_SS	U Edge Spacer, T Intermediate Spacer, 6mm Glass, 14mm Gap (Aerogel), 6mm Glass, Thermally Broken Aluminum Frame, Stainless Steel Spacer
	UHWA6146_TBAL_PVC	U Edge Spacer, H Intermediate Spacer, 6mm Glass, 14mm Gap (Aerogel), 6mm Glass, Thermally Broken Aluminum Frame, PVC Spacer
	UXWA6146_TBAL_PVC	U Edge Spacer, X Intermediate Spacer, 6mm Glass, 14mm Gap (Aerogel), 6mm Glass, Thermally Broken Aluminum Frame, PVC Spacer
	UTWA6146_TBAL_PVC	U Edge Spacer, T Intermediate Spacer, 6mm Glass, 14mm Gap (Aerogel), 6mm Glass, Thermally Broken Aluminum Frame, PVC Spacer
	Vinyl Frame	UHWA6146_Vinyl_AL
UXWA6146_Vinyl_AL		U Edge Spacer, X Intermediate Spacer, 6mm Glass, 14mm Gap (Aerogel), 6mm Glass, Vinyl Frame, Aluminum Spacer
UTWA6146_Vinyl_AL		U Edge Spacer, T Intermediate Spacer, 6mm Glass, 14mm Gap (Aerogel), 6mm Glass, Vinyl Frame, Aluminum Spacer
UHWA6146_Vinyl_SS		U Edge Spacer, H Intermediate Spacer, 6mm Glass, 14mm Gap (Aerogel), 6mm Glass, Vinyl Frame, Stainless Steel Spacer
UXWA6146_Vinyl_SS		U Edge Spacer, X Intermediate Spacer, 6mm Glass, 14mm Gap (Aerogel), 6mm Glass, Vinyl Frame, Stainless Steel Spacer
UTWA6146_Vinyl_SS		U Edge Spacer, T Intermediate Spacer, 6mm Glass, 14mm Gap (Aerogel), 6mm Glass, Vinyl Frame, Stainless Steel Spacer
UHWA6146_Vinyl_PVC		U Edge Spacer, H Intermediate Spacer, 6mm Glass, 14mm Gap (Aerogel), 6mm Glass, Vinyl Frame, PVC Spacer
UXWA6146_Vinyl_PVC		U Edge Spacer, X Intermediate Spacer, 6mm Glass, 14mm Gap (Aerogel), 6mm Glass, Vinyl Frame, PVC Spacer
UTWA6146_Vinyl_PVC		U Edge Spacer, T Intermediate Spacer, 6mm Glass, 14mm Gap (Aerogel), 6mm Glass, Vinyl Frame, PVC Spacer

Table 6 - Simulation model Identification part b

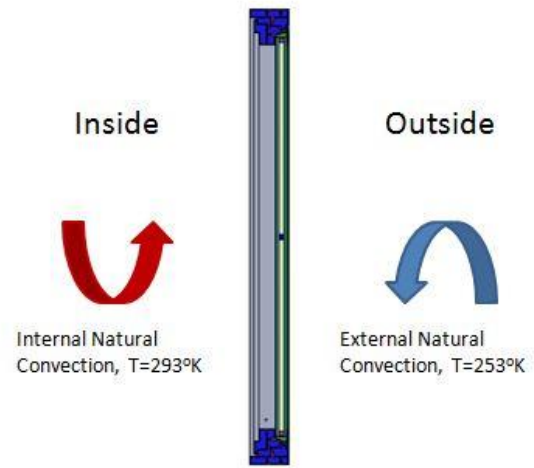
The low thermal conductivity and high solar energy transmittance of monolithic silica aerogel are beneficial qualities for passive solar heating of buildings in cold climates, potentially reducing annual energy consumption. A winter scenario was simulated where the interior face of the window experienced natural convection at a temperature of 293°K and the exterior face experienced natural convection at a temperature of 253°K. The perimeter boundary faces of the window system were

treated as adiabatic with no heat flux. The simulations do not take into account for natural convection or radiation within the cavities of the thermally broken aluminum and vinyl window frames or air cavities between the spacers and adjacent glass and aerogel panes. It was assumed that the depths of the cavities are small enough that natural convection and radiation would be negligible. The simulation only takes into account for conduction through solid objects. COMSOL has the ability to compute the conduction through liquid / gas materials. All the unvented air cavities between the spacers and aluminum and vinyl window frame were assigned this condition. The boundary conditions for the simulations are shown on Fig. 27.



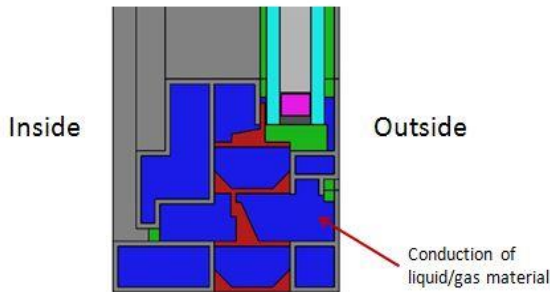
(1)

1. The perimeter boundary faces (orange) of the window were treated as adiabatic where the heat flux (W/m^2) was set to zero.



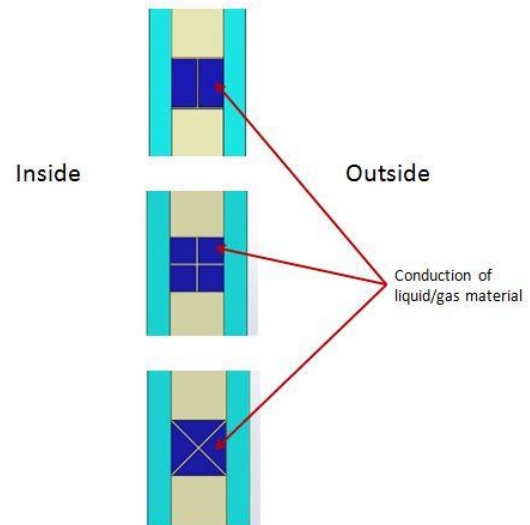
(2)

2. The internal and external faces of the window were assigned natural internal and external convection at a temperature of $293^{\circ}K$ and $253^{\circ}K$ respectively.



(3)

3. Air cavities within thermally broken aluminum and vinyl window frames were set to conduction through a liquid / gas material. The properties of air are outlined on Table 1 above.



(4)

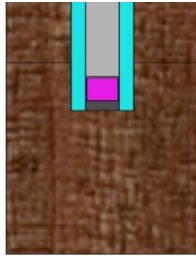
4. Air cavities between spacer and adjacent glass and aerogel panes were set to conduction through a liquid / gas material. The properties of air are outlined on Table 1 above.

Figure 27 – Boundary conditions for heat transfer analysis in COMSOL

4 Results

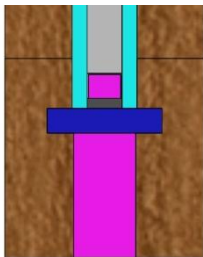
4.1 Effective Conductivity

It is difficult to conduct a 1D conduction heat transfer analysis of components with complex geometry. The effective conductivity is useful as it converts the real conductivity of the spacers and thermally broken window frames into a simple homogenous rectangular solid. The conductivity of the solid is equal to the effective conductivity of the real assembly of the spacers and thermally broken window frames and can be used to perform a 1D analysis. Figures 28 and 29 respectively provide the effective conductivities of the window frames and spacers computed by COMSOL.



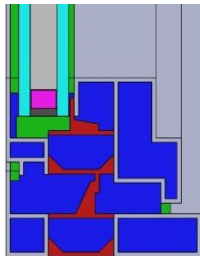
$$\lambda_{\text{eff}} = 0.12\text{W/mK}$$

Solid Wood Window Frame



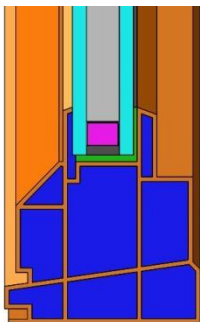
$$\lambda_{\text{eff}} = 0.101\text{W/mK}$$

Thermally Broken Wooden Window Frame



$$\lambda_{\text{eff}} = 26.23\text{W/mK}$$

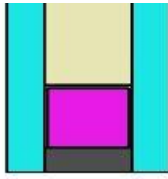
Thermally Broken Aluminum Window Frame



$$\lambda_{\text{eff}} = 0.062\text{W/mK}$$

Vinyl Window Frame

Figure 28 – Effective conductivity of window frames (λ_{eff})

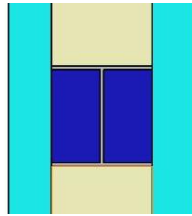


'U' Edge Spacer

$$\lambda_{\text{eff}}(\text{AL}) = 18.82\text{W/mK}$$

$$\lambda_{\text{eff}}(\text{SS}) = 1.79\text{W/mK}$$

$$\lambda_{\text{eff}}(\text{PVC}) = 0.046\text{W/mK}$$

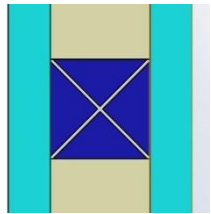


'H' Intermediate Spacer

$$\lambda_{\text{eff}}(\text{AL}) = 16.76\text{W/mK}$$

$$\lambda_{\text{eff}}(\text{SS}) = 1.59\text{W/mK}$$

$$\lambda_{\text{eff}}(\text{PVC}) = 0.042\text{W/mK}$$

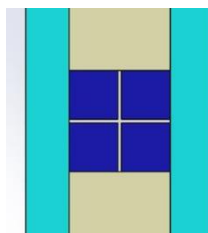


'X' Intermediate Spacer

$$\lambda_{\text{eff}}(\text{AL}) = 15.84\text{W/mK}$$

$$\lambda_{\text{eff}}(\text{SS}) = 1.51\text{W/mK}$$

$$\lambda_{\text{eff}}(\text{PVC}) = 0.041\text{W/mK}$$



'T' Intermediate Spacer

$$\lambda_{\text{eff}}(\text{AL}) = 11.29\text{W/mK}$$

$$\lambda_{\text{eff}}(\text{SS}) = 1.079\text{W/mK}$$

$$\lambda_{\text{eff}}(\text{PVC}) = 0.037\text{W/mK}$$

Figure 29 – Effective conductivity of spacers (λ_{eff})

4.2 U-Value of Window Systems

A 1D analysis was initially performed to determine the overall performance of each window system. An area weighted U-value calculation was performed, using the effective conductivities computed by COMSOL. Figures 30 plots the U-values of the solid wood, thermally broken wooden, thermally broken aluminum, and vinyl framed monolithic aerogel insulated window systems.

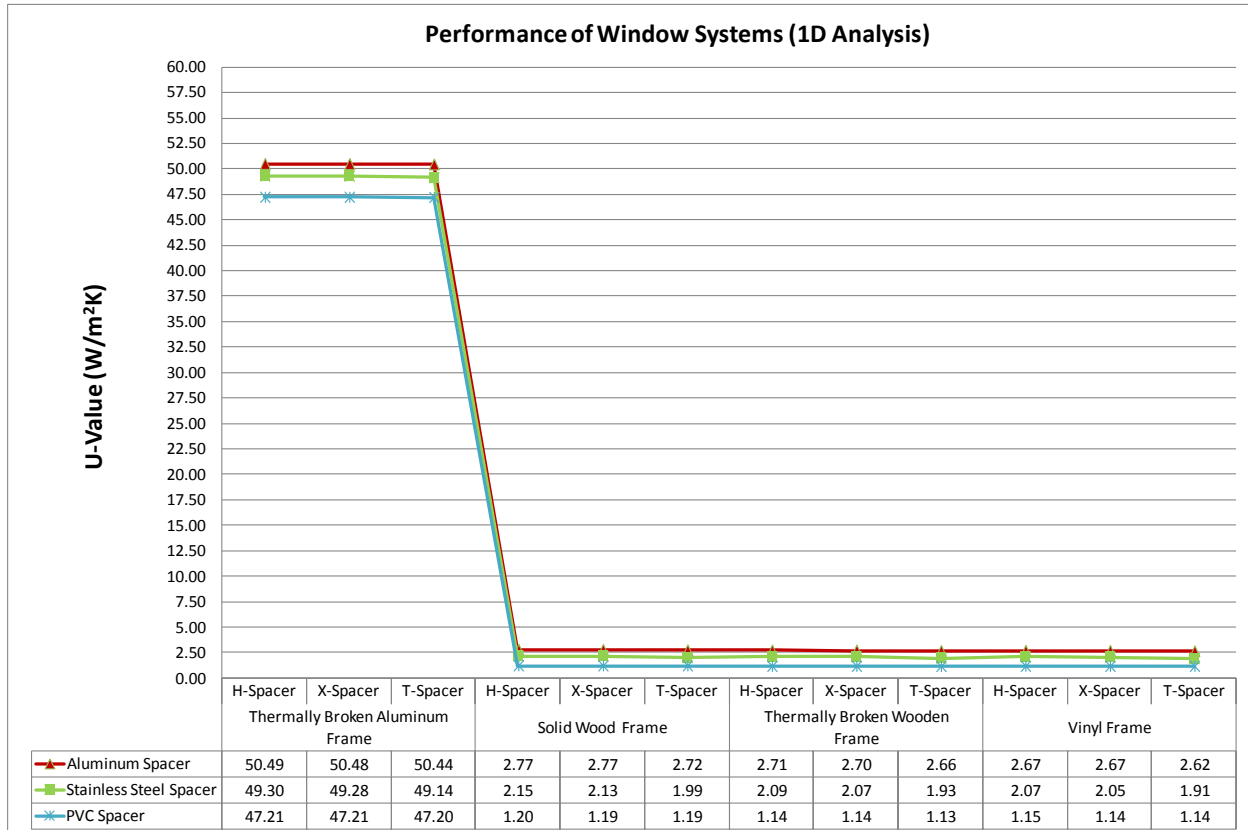


Figure 30 – Performance of Window Systems (3D Analysis)

The results shown on Fig. 30 indicate that the geometry of the spacer has less effect on the performance compared to the material of construction. For all materials of construction, the 'H' and 'X' spacer perform about the same while the 'T' spacer shows a moderately improved performance. The effective conductivity of PVC spacers is much less compared to aluminum and stainless steel spacers. The best performing window system analyzed in 1D, having a U-value of 1.13W/m²k was the thermally broken wooden framed window with 'T' intermediate and 'U' shaped edge spacers made of PVC. The thermally broken wooden framed window systems perform better compared to the solid wood framed window

systems. The thermal break reduces the thermal bridging at the window frame, reducing the U values by approximately 2% to 5%. The U-values of the thermally broken aluminum window systems is much higher compared to the U-values of the windows modelled with solid, thermally broken wooden, and vinyl frames, potentially illustrating the limitation of relying on a 1D analysis. A better approach for determining the U-value for the window systems involved taking advantage of the 3D finite element heat transfer analysis by COMSOL and using the heat flux generated for each simulation. Using the heat flux computed by COMSOL, and solving for the U-value, the equation governing heat transfer by conduction was rearranged as shown below.

$$Q_{\text{cond}} / A = U \times (T_2 - T_1) \quad [5]$$

Where,

Q_{cond} / A is the heat flux in (W/m^2)

Table 7 shows the heat flux values computed by the COMSOL's finite element heat transfer analysis. Figure 31 plots the U-values of the solid wood, thermally broken wooden, thermally broken aluminum, and vinyl framed window systems insulated with monolithic silica aerogel. The U-values were calculated using the heat flux values generated by the COMSOL simulations.

Solid Wood Frame Monolithic Aerogel Insulated Window System	
Model #	Heat Flux (W/m²)
UHWA6146_W_AL	74.97
UXWA6146_W_AL	76.21
UTWA6146_W_AL	71.91
UHWA6146_W_SS	65.54
UXWA6146_W_SS	66.04
UTWA6146_W_SS	62.03
UHWA6146_W_PVC	45.91
UXWA6146_W_PVC	45.81
UTWA6146_W_PVC	45.58
Thermally Broken Wooden Frame Monolithic Aerogel Insulated Window System	
Model #	Heat Flux (W/m²)
UHWA6146_TBW_AL	70.67
UXWA6146_TBW_AL	71.89
UTWA6146_TBW_AL	67.47
UHWA6146_TBW_SS	60.35
UXWA6146_TBW_SS	60.38
UTWA6146_TBW_SS	57.22
UHWA6146_TBW_PVC	39.70
UXWA6146_TBW_PVC	39.59
UTWA6146_TBW_PVC	39.36
Thermally Broken Aluminum Frame Monolithic Aerogel Insulated Window System	
Model #	Heat Flux (W/m²)
UHWA6146_TBAL_AL	83.51
UXWA6146_TBAL_AL	84.26
UTWA6146_TBAL_AL	80.55
UHWA6146_TBAL_SS	73.78
UXWA6146_TBAL_SS	74.11
UTWA6146_TBAL_SS	71.06
UHWA6146_TBAL_PVC	56.57
UXWA6146_TBAL_PVC	56.72
UTWA6146_TBAL_PVC	56.66
Vinyl Frame Monolithic Aerogel Insulated Window System	
Model #	Heat Flux (W/m²)
UHWA6146_Vinyl_AL	66.15
UXWA6146_Vinyl_AL	67.31
UTWA6146_Vinyl_AL	62.94
UHWA6146_Vinyl_SS	56.92
UXWA6146_Vinyl_SS	57.33
UTWA6146_Vinyl_SS	53.66
UHWA6146_Vinyl_PVC	37.03
UXWA6146_Vinyl_PVC	36.85
UTWA6146_Vinyl_PVC	36.66

Table 7 - Heat flux (W/m²) for window systems computed by COMSOL

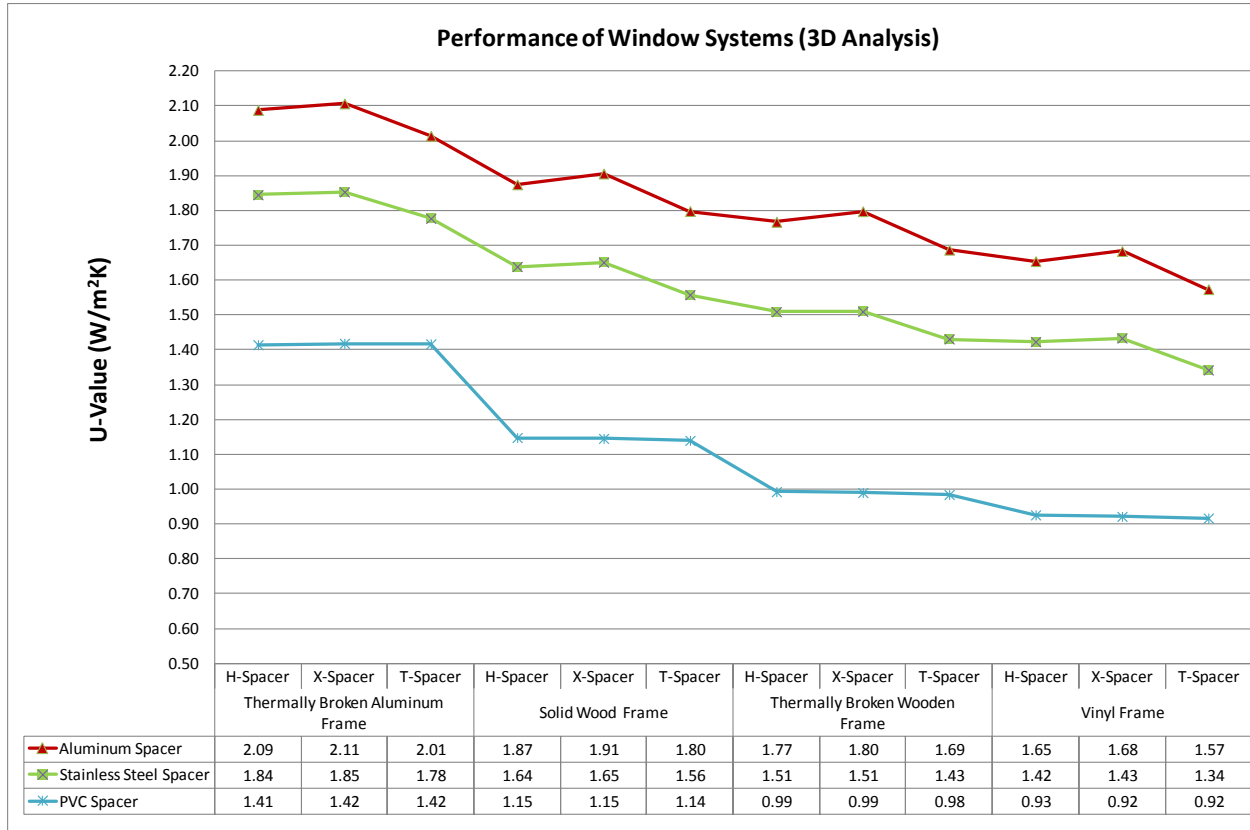


Figure 31 – Performance of Window Systems (3D Analysis)

The best performing window system analyzed in 3D was the vinyl framed window with ‘T’ intermediate and ‘U’ shaped edge spacers made of PVC. The U-value was 0.92W/m²k, which is a 19.6% improvement compared to the same window system analyzed in 1D. The 3D analysis also confirms that the material of construction positively influences the performance of the aerogel insulated window system more than the geometry of the spacer. Generally the ‘T’ spacer made of aluminum and stainless steel performs better when compared to the ‘H’ and ‘X’ spacers made of the same respective materials. However, the ‘T’ spacer made of PVC only performs marginally better compared to the ‘H’ and ‘X’ spacer made of PVC, suggesting that the spacer geometry only impacts the thermal performance when conductive materials are used. However, as the material conductivity decreases, the U-value converges and becomes constant regardless of the spacer geometry.

For the solid wood framed window systems, the best performing spacer geometry improves the U-value from 0.7% to 5.7%, depending on the material of construction. However, the material of construction improves the U-value from 36.6% to 39.9%, depending on the spacer geometry. For the thermally

broken wooden framed window systems, the best performing spacer geometry improves the U-value from 0.8% to 6.1%, depending on the material of construction. However, the material of construction improves the U-value from 41.7% to 44.9%, depending on the spacer geometry. The performance of the thermally broken wooden framed window systems analyzed in 3D improve by 6% to 14% compared to the solid wood framed window systems, depending on the spacers geometry and its material of construction. For the vinyl framed window systems, the best performing spacer geometry improves the U-value from 1% to 6.5%, depending on the material of construction. However, the material of construction improves the U-value from 41.8% to 45.3%, depending on the spacer geometry. For the thermally broken aluminum framed window systems, the best performing spacer geometry improves the U-value from 0.3% to 4.4%, depending on the material of construction. However, the material of construction improves the U-value from 29.7% to 32.7%, depending on the spacer geometry.

In general, the thermally broken aluminum window framed systems performed the poorest when compared to the other window systems. However, the results cannot be generalized because the window frame that was modelled may not necessarily be the most efficient frame available on the market. The cavity depths exceed the optimal depth of 20mm (Asdrubali, 2013), which could be impacting the performance. Although natural convection and radiation heat transfer modes were not included in the analysis, increasing the number of unvented air cavities and using surface treatments that reduce the surface emissivity would respectively reduce the convection and radiation coefficients, inherently increasing the thermal resistance of the frame. However, considering the relative performance of the window systems assessed, the thermally broken aluminum frame could be better suited for larger windows. Increasing the glazing area will proportionally reduce the impact the frame will have on the overall U-value of the window system, bettering its holistic performance

The vinyl framed window systems performed relatively better compared to the other window frames accessed. Table 8 compares the performance of the vinyl framed aerogel window to a double glazed window with the same window frame type but an interpane space filled with air.

Vinyl Framed Window Systems			
Model #	U-value of Aerogel Insulated Window	U-value of Aerogel Insulated Window	% Variation
UHWA6146_Vinyl_AL	1.65	1.73	-4.6%
UXWA6146_Vinyl_AL	1.68	1.76	-4.5%
UTWA6146_Vinyl_AL	1.57	1.66	-5.1%
UHWA6146_Vinyl_SS	1.42	1.51	-5.6%
UXWA6146_Vinyl_SS	1.43	1.53	-6.0%
UTWA6146_Vinyl_SS	1.34	1.44	-6.9%
UHWA6146_Vinyl_PVC	0.93	1.07	-13.1%
UXWA6146_Vinyl_PVC	0.92	1.07	-13.6%
UTWA6146_Vinyl_PVC	0.92	1.06	-13.8%

Table 8 – Comparing performance of aerogel insulated window with air filled double glazed window

The aerogel insulated window improves the U-value from 4.5% to 13.8% compared to the same double glazed window with an air cavity. The magnitude of the percentage variation increases as the effective conductivity of the spacer decreases. The aluminum and stainless steel spacers marginally reduce the U-value from 4.5% to 6.9%. However, the PVC spacers have the lowest effective conductivity of all spacers assessed and they improve the U-value from 13.1% to 13.8%. In order to make a stronger case for aerogel insulated windows, low conductive edge and intermediate spacers should be used to better the performance compared to less efficient window systems.

The 3D analysis improved the U-value by as much as 97% compared to the 1D analysis. Table 9 shows the percentage variation in U-value, comparing the results obtained from the 1D and 3D heat transfer analysis.

Solid Wood Frame Monolithic Aerogel Insulated Window System			
Model #	U-Value (W/m²k) 1D Analysis	U-Value (W/m²k) 3D Analysis	% Variations
UHWA6146_W_AL	2.77	1.87	-32.33%
UXWA6146_W_AL	2.77	1.91	-31.22%
UTWA6146_W_AL	2.72	1.80	-33.91%
UHWA6146_W_SS	2.15	1.64	-23.79%
UXWA6146_W_SS	2.13	1.65	-22.49%
UTWA6146_W_SS	1.99	1.56	-21.73%
UHWA6146_W_PVC	1.20	1.15	-4.36%
UXWA6146_W_PVC	1.19	1.15	-3.77%
UTWA6146_W_PVC	1.19	1.14	-4.25%
Thermally Broken Wooden Frame Monolithic Aerogel Insulated Window System			
Model #	U-Value (W/m²k) 1D Analysis	U-Value (W/m²k) 3D Analysis	% Variations
UHWA6146_TBW_AL	2.71	1.77	-34.81%
UXWA6146_TBW_AL	2.70	1.80	-33.44%
UTWA6146_TBW_AL	2.66	1.69	-36.59%
UHWA6146_TBW_SS	2.09	1.51	-27.81%
UXWA6146_TBW_SS	2.07	1.51	-27.07%
UTWA6146_TBW_SS	1.93	1.43	-25.88%
UHWA6146_TBW_PVC	1.14	0.99	-12.95%
UXWA6146_TBW_PVC	1.14	0.99	-13.18%
UTWA6146_TBW_PVC	1.13	0.98	-12.92%
Thermally Broken Aluminum Frame Monolithic Aerogel Insulated Window System			
Model #	U-Value (W/m²k) 1D Analysis	U-Value (W/m²k) 3D Analysis	% Variations
UHWA6146_TBAL_AL	50.49	2.09	-95.86%
UXWA6146_TBAL_AL	50.48	2.11	-95.83%
UTWA6146_TBAL_AL	50.44	2.01	-96.01%
UHWA6146_TBAL_SS	40.30	1.84	-95.42%
UXWA6146_TBAL_SS	49.28	1.85	-96.24%
UTWA6146_TBAL_SS	49.14	1.78	-96.38%
UHWA6146_TBAL_PVC	47.21	1.41	-97.00%
UXWA6146_TBAL_PVC	47.21	1.42	-97.00%
UTWA6146_TBAL_PVC	47.20	1.42	-97.00%
Vinyl Frame Monolithic Aerogel Insulated Window System			
Model #	U-Value (W/m²k) 1D Analysis	U-Value (W/m²k) 3D Analysis	% Variations
UHWA6146_Vinyl_AL	2.67	1.65	-38.06%
UXWA6146_Vinyl_AL	2.67	1.68	-36.97%
UTWA6146_Vinyl_AL	2.62	1.57	-39.94%
UHWA6146_Vinyl_SS	2.07	1.42	-31.26%
UXWA6146_Vinyl_SS	2.05	1.43	-30.09%
UTWA6146_Vinyl_SS	1.91	1.34	-29.76%
UHWA6146_Vinyl_PVC	1.15	0.93	-19.50%
UXWA6146_Vinyl_PVC	1.14	0.92	-19.81%
UTWA6146_Vinyl_PVC	1.14	0.92	-19.61%

Table 9 – U-value (W/m²k) comparison of results between 1D and 3D analysis

Depending on the spacer geometry it's material of construction and window frame type, the U-values generated from the 3D analysis improve anywhere from 3.8% to 97% compared to the U-values

calculated in the 1D analysis, demonstrating the advantage and relevance of a 3D finite element heat transfer analysis.

Table 10 shows the heat flux (W/m^2) of the frameless glazing units computed by the COMSOL's finite element heat transfer analysis. Figure 32 is an illustration of the 1040mm x 1040mm frameless glazing unit.

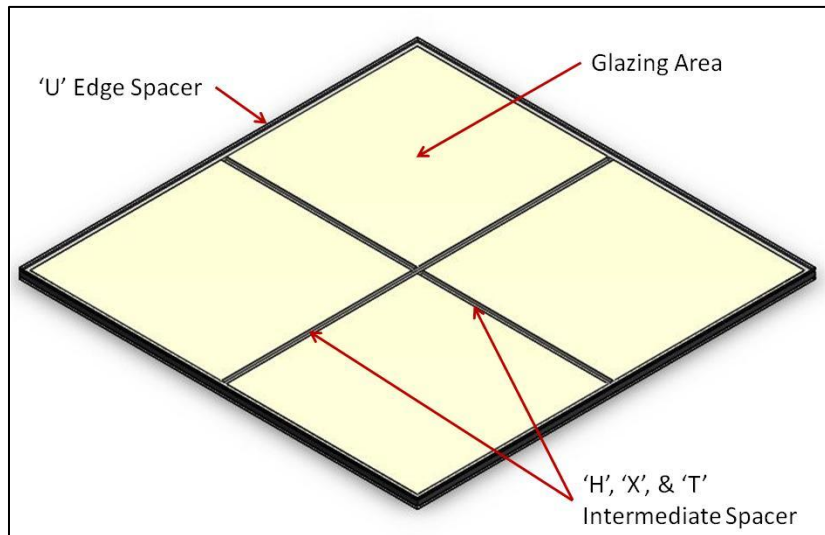


Figure 32 – Illustration of frameless glazing

Glazing with Aluminum Spacers (No Frame)		
Model #	Heat Flux (W/m^2)	U-Value (W/m^2k)
UHWA6146_AL	102.20	2.56
UXWA6146_AL	104.54	2.61
UTWA6146_AL	96.37	2.41
Glazing with Stainless Steel Spacers (No Frame)		
Model #	Heat Flux (W/m^2)	U-Value (W/m^2k)
UHWA6146_SS	85.18	2.13
UXWA6146_SS	86.125	2.15
UTWA6146_SS	79.183	1.98
Glazing with PVC Spacers (No Frame)		
Model #	Heat Flux (W/m^2)	U-Value (W/m^2k)
UHWA6146_PVC	49.04	1.23
UXWA6146_PVC	48.84	1.22
UTWA6146_PVC	48.41	1.21

Table 10 - Heat flux (W/m^2) and U-value (W/m^2k) for frameless glazing computed by COMSOL

You would normally expect more heat to escape from the more conductive window frame. However, the heat flux of the frameless glazing units are higher compared to the heat flux of the 36 window systems modelled in COMSOL. Depending on the spacer geometry and its materials of construction and window frame type, the U-values of the glazing units are approximately 5.4% to 39.9% greater compared to the U-values of the window systems analyzed in COMSOL. Most of the heat is lost around the perimeter insulated 'U' edge spacer in the glazing unit. However, as illustrated on Fig. 26, 20mm of the glazing unit including the insulated 'U' edge spacer is protected by the window frame, increasing thermal resistance. Furthermore, the added area and depth of the window frame improves the overall thermal performance of the window systems.

4.3 Centre of Glass, Edge of Glass, and Window Frame Segments

A key energy strategy for window frames is to use low conductivity materials and components, which would minimize the edge of glass band and the thermal transmittance through a window, decreasing heat loss from the warm interior space to the colder exterior during winter months, and vice versa during summer months. Therefore the design of each single component of a window becomes an important task. Figure 33 shows the percentage of each segment for the 36 window systems modelled. For the solid wood and thermally broken wooden framed window systems, the window frame segment is 26%. Therefore the maximum centre of glass region can be 74%. The window frame segment is 29.3% for the thermally broken aluminum window frame, allowing a maximum centre of glass region of 70.7%. For the vinyl framed window system, the window frame segment is 28%, allowing a maximum centre of glass region of 72%.

Centre of Glass, Edge of Glass, & Window Frame Proportion Percentages

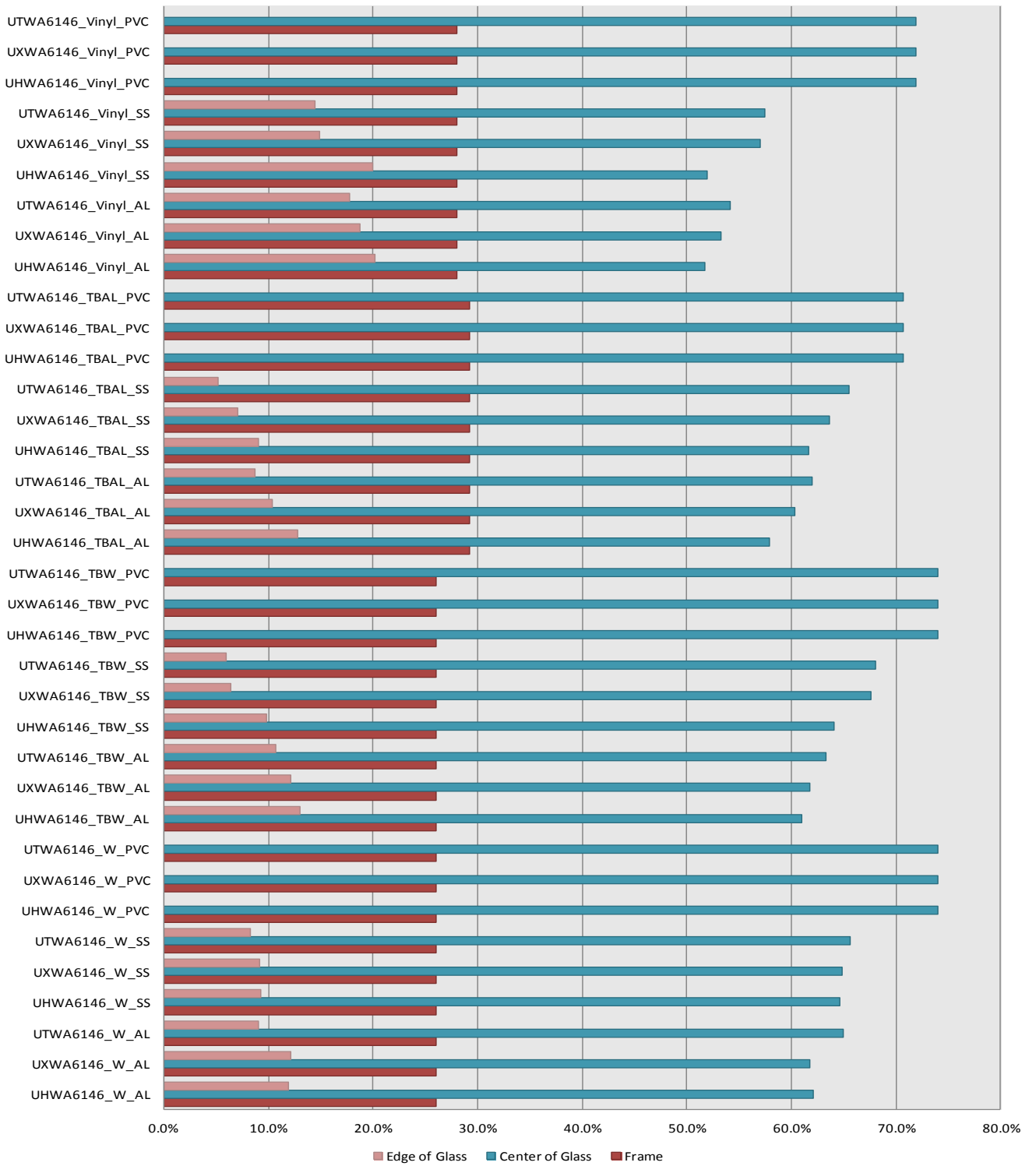


Figure 33 – Centre of glass, edge of glass, and window frame segment percentages

The results on Fig. 33 suggest that regardless of the geometry, all window systems using PVC spacers have the maximum centre of glass region. The effective conductivity of the 'H', 'X', and 'T' spacers made of PVC is 0.042W/mK, 0.041W/mK, 0.037W/mK respectively. These effective conductivities are close to the conductivity of monolithic silica aerogel (0.015W/mK), minimizing the thermal bridging at the intermediate and edge of glass region compared to the aluminum and stainless steel spacers. The PVC spacers result in decreased heat loss from the warm interior to the cold exterior.

4.4 Thermographic Heat Transfer Diagram

In a 1D analysis, the assumption is that the heat transfer path is unidirectional, not fully taking into account for the effects of a thermal break, which changes and lengthens the heat transfer path, inherently improving the performance of a window system. Figures 34, 35, 36, and 37 respectively show the thermographic heat transfer diagrams for the poor and better performing solid wood, thermally broken wooden, thermally broken aluminum, and vinyl framed window systems. The diagrams below showcases the advantage of a 3D finite element heat transfer analysis, demonstrating how the heat transfer is not unidirectional and in fact takes on a three dimensional path avoiding low conductive thermal breaks.

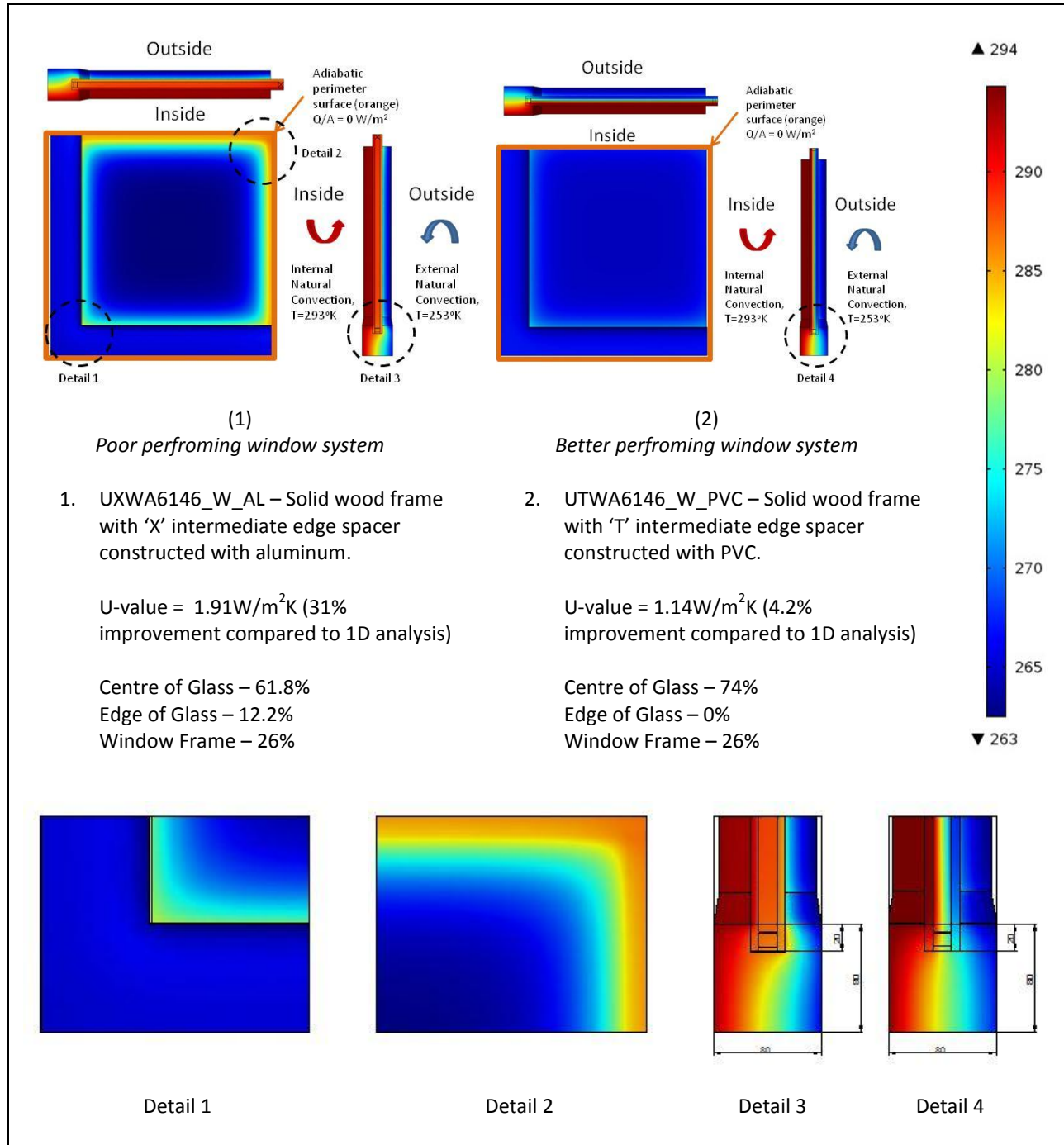


Figure 34 – Thermographic heat transfer diagram (Solid Wood Window)

Detail 1 on Fig. 34 indicates that the exterior side of solid wood frame is at a temperature closer to the exterior conditions ($253^\circ\text{K} < T_{\text{ext}} < 265^\circ\text{K}$), while detail 2 shows signs of thermal bridging on the exterior glass pane along the aluminum intermediate ‘X’ spacer, where temperature is closer to the interior condition ($275^\circ\text{K} < T_{\text{ext}} < 285^\circ\text{K}$). Detail 3 suggests that the heat transfer through the solid wood frame is

slow and that the heat is migrating upwards and escaping through the more conductive 'U' edge spacer. The U-value of the solid wood framed window system with 'X' intermediate and 'U' edge spacers made of aluminum is $1.91\text{W/m}^2\text{k}$. The effective conductivity of the 'U' edge spacer made of aluminum is 18.82W/mK , explaining the thermal bridging and heat loss shown on detail 1 along the edge of the exterior glass pane just above the window frame. The centre of glass region is at 61.8% while the edge of glass region is at 12.2%.

Detail 4 shows how the improved geometry of the intermediate 'T' spacer and thermal performance of both the intermediate and 'U' edge spacer made of PVC slows down the overall heat transfer through the window system. The 'U' edge and 'T' intermediate spacer made of PVC with effective conductivities of 0.046W/mK and 0.037W/mK respectively reduce the U-value of the window system by approximately 40% compared to the poor performing solid wood framed window system with 'X' intermediate and 'U' edge spacers made of aluminum. Detail 4 shows distinct vertical temperature bands, suggesting gradual heat loss through the window system. The exterior glass pane and window frame are at a temperature near the exterior condition ($265^\circ\text{K} < T_{\text{ext}} < 270^\circ\text{K}$), explaining the improved performance of the solid wood framed window system with 'T' intermediate and 'U' edge spacers made of PVC. The centre of glass region is at the maximum 74%, visually indicating no significant thermal bridging in the better performing window system.

Thermographic heat transfer diagrams for the remaining solid wood framed window systems may be seen on Appendix 1.

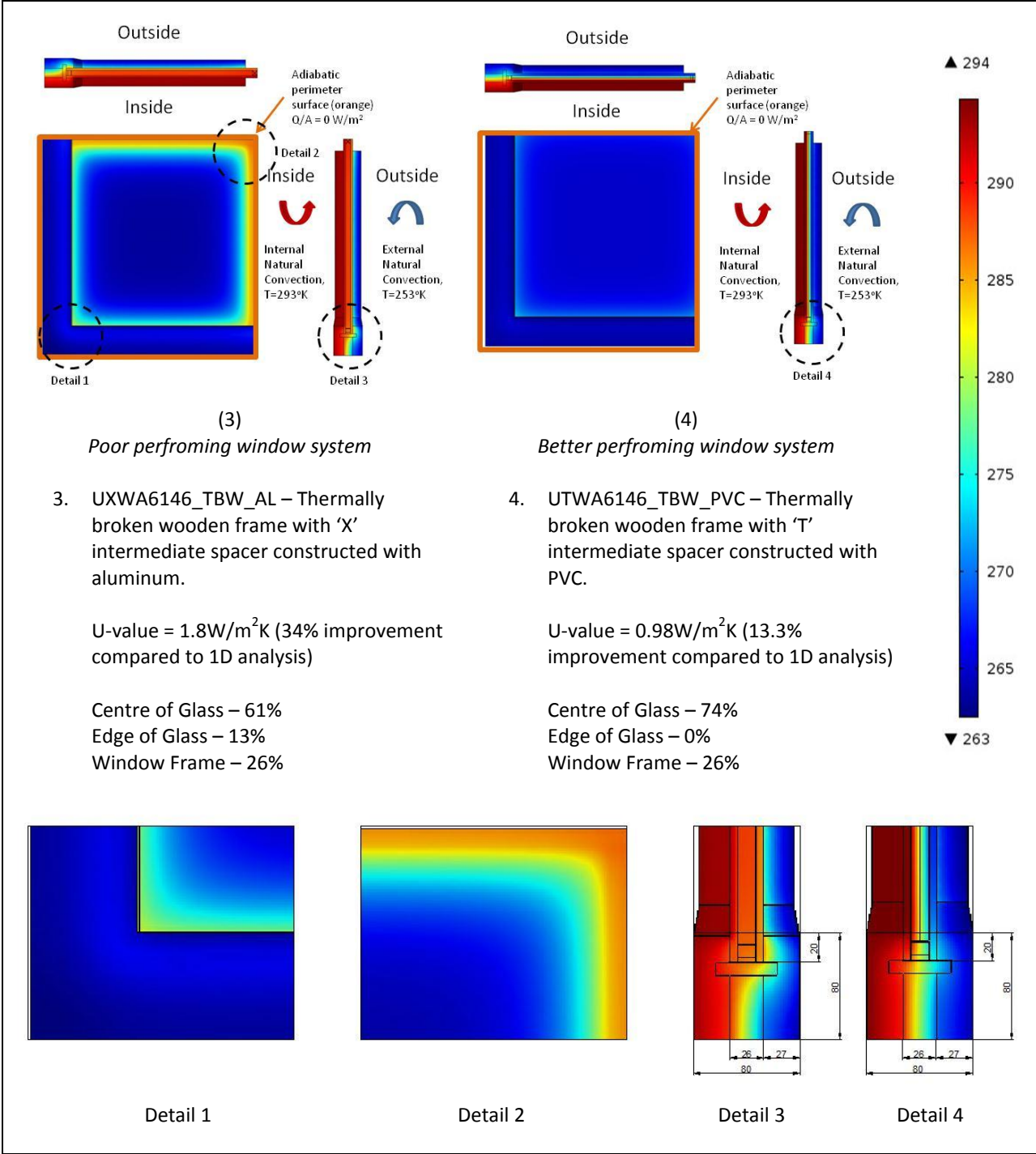


Figure 35 – Thermographic heat transfer diagram (Thermally Broken Wooden Window)

Detail 1 on Fig. 35 indicates that the exterior side of the thermally broken wooden frame is at a temperature closer to the exterior conditions ($253^\circ\text{K} < T_{\text{ext}} < 265^\circ\text{K}$), while detail 2 shows signs of thermal bridging on the exterior glass pane along the aluminum intermediate ‘X’ spacer, where

temperature is closer to the interior condition ($275^{\circ}\text{K} < T_{\text{ext}} < 285^{\circ}\text{K}$).--The effective conductivity of the thermally broken wooden window frame is 0.101W/mK , approximately 16% less than the solid wood frame. The thermal break slows down the heat transfer through the window frame allowing more heat to migrate upward and escape through the more conductive 'U' edge spacer. The thermal break marginally reduces the centre of glass region to 61%, increasing the edge of glass region to 13% when compared to the solid wood framed window system with the same spacer geometry and material of construction. The effective conductivity of the 'U' edge spacer made of aluminum is 18.82W/mK , explaining the thermal bridging and heat loss shown on detail 1 along the edge of the exterior glass pane just above the window frame.

Detail 4 shows how the improved geometry of the intermediate 'T' spacer and thermal performance of both the intermediate and 'U' edge spacer made of PVC slows down the overall heat transfer through the window system. The 'U' edge and 'T' intermediate spacer made of PVC with effective conductivities of 0.046W/mK and 0.037W/mK respectively reduce the U-value of the window system by approximately 46% compared to the poor performing thermally broken wooden framed window system with 'X' intermediate and 'U' edge spacers made of aluminum. Detail 4 shows distinct vertical temperature bands, suggesting gradual heat loss through the window system. The exterior glass pane and window frame are at a temperature near the exterior condition ($265^{\circ}\text{K} < T_{\text{ext}} < 270^{\circ}\text{K}$), explaining the improved performance of the thermally broken wooden framed window system with 'T' intermediate and 'U' edge spacers made of PVC. The centre of glass region is at the maximum 74%, visually indicating no significant thermal bridging in the better performing window system.

Thermographic heat transfer diagrams for the remaining thermally broken wooden framed window systems may be seen on Appendix 1.

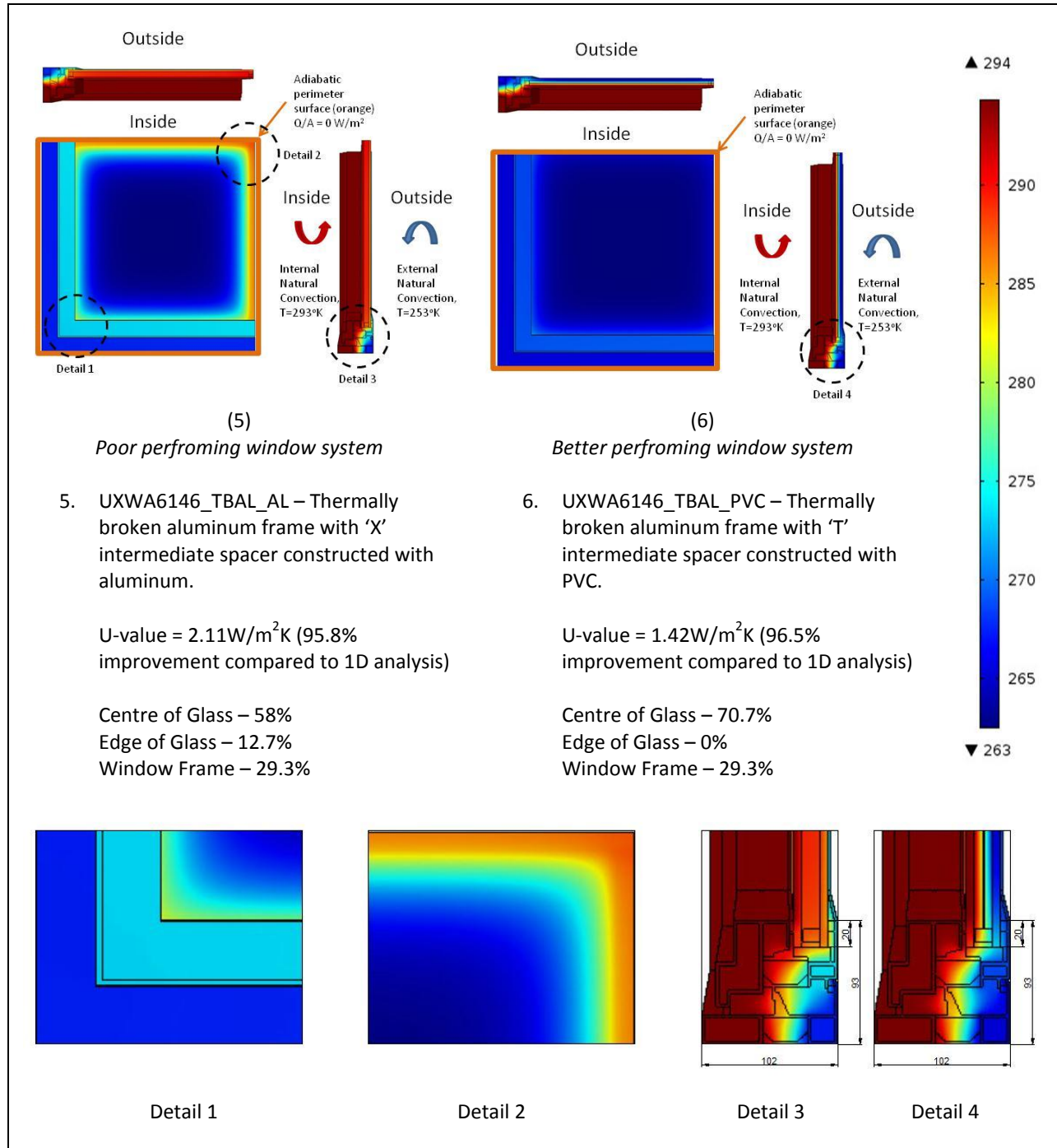


Figure 36 – Thermographic heat transfer diagram (Thermally Broken Aluminum Window)

Detail 1 on Fig. 36 indicates that the exterior side of the thermally broken aluminum frame is at a temperature greater than the exterior condition ($265^{\circ}\text{K} < T_{\text{ext}} < 275^{\circ}\text{K}$), while detail 2 shows signs of thermal bridging on the exterior glass pane along the aluminum intermediate ‘X’ spacer, where temperature is closer to the interior condition ($275^{\circ}\text{K} < T_{\text{ext}} < 285^{\circ}\text{K}$). The effective conductivity of the

thermally broken aluminum frame is 26.23W/mK. However, the polyamide thermal break slows down the heat transfer through the window frame allowing more heat to migrate upward and escape through the conductive 'U' edge spacer. The effective conductivity of the 'U' edge spacer made of aluminum is 18.82W/mK, explaining the thermal bridging and heat loss shown on detail 1 along the edge of the exterior glass pane just above the window frame. The wider window frame reduces the centre of glass region to 58% while the edge of glass region is at 12.7%.

Detail 4 shows how the improved geometry of the intermediate 'T' spacer and thermal performance of both the intermediate and 'U' edge spacer made of PVC slows down the overall heat transfer through the window system. The 'U' edge and 'T' intermediate spacer made of PVC with effective conductivities of 0.046W/mK and 0.037W/mK respectively reduce the U-value of the window system by approximately 33% compared to the poor performing thermally broken aluminum framed window system with 'X' intermediate and 'U' edge spacers made of aluminum. Detail 4 shows distinct vertical temperature bands, suggesting gradual heat loss through the window system. The exterior glass pane and window frame are at a temperature near the exterior condition ($265^{\circ}\text{K} < T_{\text{ext}} < 270^{\circ}\text{K}$), explaining the improved performance of the thermally broken aluminum framed window system with 'T' intermediate and 'U' edge spacers made of PVC. The centre of glass region is at the maximum 70.7%, visually indicating no significant thermal bridging in the better performing window system.

Thermographic heat transfer diagrams for the remaining thermally broken aluminum framed window systems may be seen on Appendix 1.

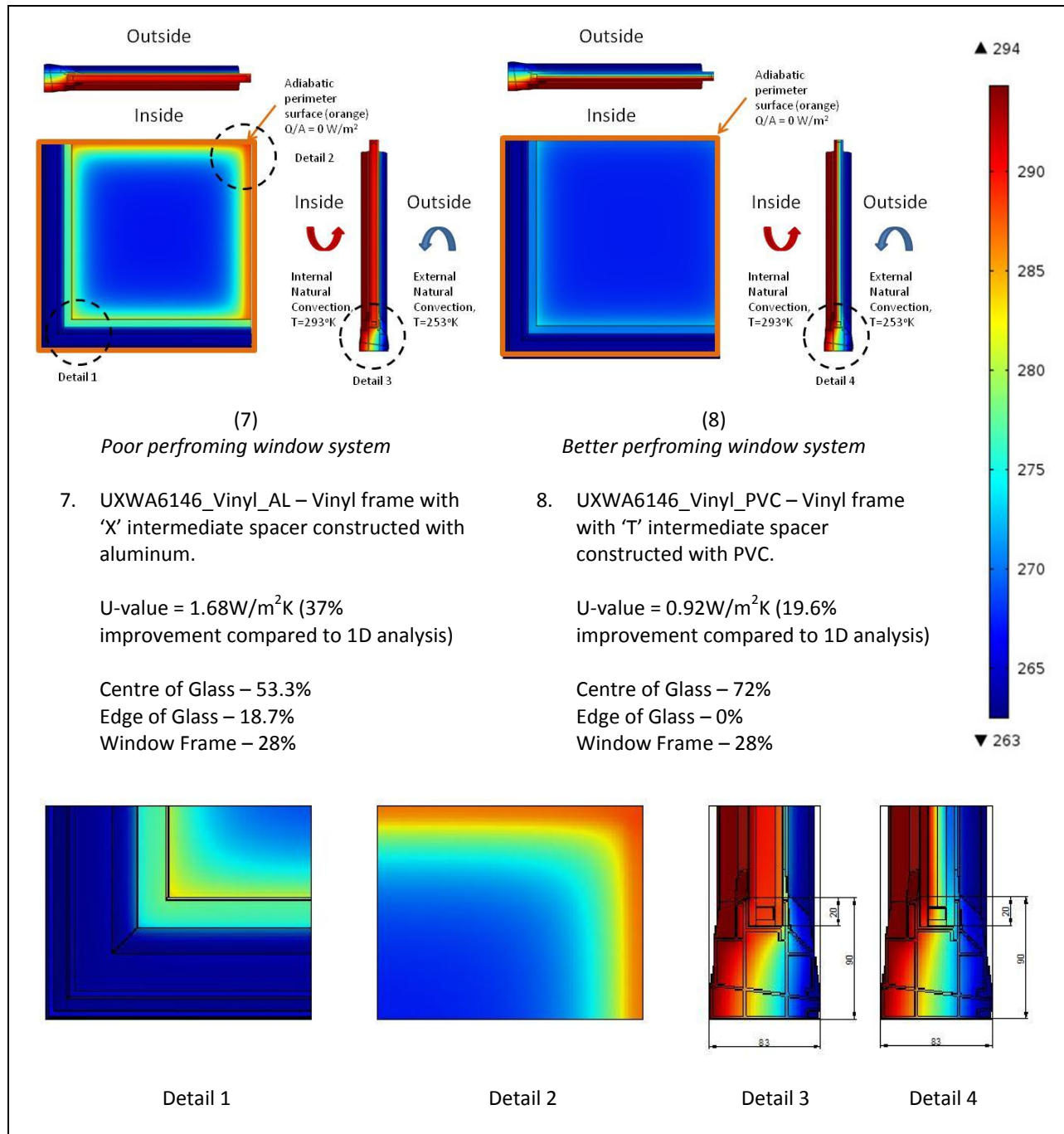


Figure 37 – Thermographic heat transfer diagram (Vinyl Window)

Detail 1 on Fig. 37 indicates that the exterior side of the vinyl frame is at a temperature greater than the exterior condition ($265^\circ\text{K} < T_{\text{ext}} < 275^\circ\text{K}$), while detail 2 shows signs of thermal bridging on the exterior glass pane along the aluminum intermediate 'X' spacer, where temperature is closer to the interior condition ($275^\circ\text{K} < T_{\text{ext}} < 285^\circ\text{K}$).

The effective conductivity of the 'U' edge spacer made of aluminum is 18.82W/mK, explaining the thermal bridging and heat loss shown on detail 1 along the edge of the exterior glass pane just above the window frame. The wider window frame reduces the centre of glass region contribution to 53.3% while the edge of glass region is at 18.7%.

Detail 4 shows how the improved geometry of the intermediate 'T' spacer and thermal performance of both the intermediate and 'U' edge spacer made of PVC slows down the overall heat transfer through the window system. The 'U' edge and 'T' intermediate spacer made of PVC with effective conductivities of 0.046W/mK and 0.037W/mK respectively reduce the U-value of the window system by approximately 45% compared to the poor performing thermally broken aluminum framed window system with 'X' intermediate and 'U' edge spacers made of aluminum. Detail 4 shows distinct vertical temperature bands, suggesting gradual heat loss through the window system. The exterior glass pane and window frame are at a temperature near the exterior condition ($265^{\circ}\text{K} < T_{\text{ext}} < 270^{\circ}\text{K}$), explaining the improved performance of the vinyl framed window system with 'T' intermediate and 'U' edge spacers made of PVC. The centre of glass region is at the maximum 72%, visually indicating no significant thermal bridging in the better performing window system.

Thermographic heat transfer diagrams for the remaining vinyl framed window systems may be seen on Appendix 1.

5 Discussion and Conclusion

The research focused on investigating thermal bridging at the edge and intermediate spacers dividing the French style window insulated with monolithic silica aerogel. The geometry and material of construction of the spacers was analyzed to determine which spacer system coupled with the modelled window frame effectively reduces the edge of glass region, improving the performance of the window system. Aluminum, stainless steel, and polyvinyl chloride (PVC) were the materials assigned to the spacers. A 3D finite element heat transfer analysis was undertaken using COMSOL Multiphysics, which determined that the spacer geometry improves the U-value of the window systems from 0.3% to 6.5% depending on the material of construction and window frame type. The material of construction improved the U-value of the window systems from 29.7% to 45.2% depending on the spacer geometry and window frame type. The results concluded that the best performing window system with a U-value of $0.92\text{W/m}^2\text{k}$ is a vinyl framed window system with 'T' intermediate and 'U' edge spacer made of PVC. Table 11 summarizes the results of the 36 simulations, showing the U-value and glazing segment percentages (i.e. centre of glass, edge of glass, and window frame regions) for the modelled window systems insulated with monolithic aerogel. Although vinyl framed window systems performed better, the results cannot be necessarily generalized. In this case, relative performance is more important because of differences in design, detailing, and manufacturing processes of the window frames that were modelled for this research paper.

Frame Type	Spacer Geometry	Aluminum Spacer		Stainless Steel Spacer		PVC Spacer		% Variation
		U-Value (W/m ² k)	Glazing Segment Proportion %	U-Value (W/m ² k)	Glazing Segment Proportion %	U-Value (W/m ² k)	Glazing Segment Proportion %	
Solid Wood Frame	H-Spacer	1.87	Centre of Glass – 62.1% Edge of Glass – 11.9% Window Frame – 26%	1.64	Centre of Glass – 64.7% Edge of Glass – 9.3% Window Frame – 26%	1.15	Centre of Glass – 74% Edge of Glass – 0% Window Frame – 26%	-38.8%
	X-Spacer	1.91	Centre of Glass – 61.8% Edge of Glass – 12.2% Window Frame – 26%	1.65	Centre of Glass – 64.8% Edge of Glass – 9.2% Window Frame – 26%	1.15	Centre of Glass – 74% Edge of Glass – 0% Window Frame – 26%	-39.9%
	T-Spacer	1.80	Centre of Glass – 65% Edge of Glass – 9% Window Frame – 26%	1.56	Centre of Glass – 65.7% Edge of Glass – 8.3% Window Frame – 26%	1.14	Centre of Glass – 74% Edge of Glass – 0% Window Frame – 26%	-36.6%
	% Variation	-5.6%		-5.7%		-0.7%		
Thermally Broken Wooden Frame	H-Spacer	1.77	Centre of Glass – 61% Edge of Glass – 13% Window Frame – 26%	1.51	Centre of Glass – 64.1% Edge of Glass – 9.8% Window Frame – 26%	0.99	Centre of Glass – 74% Edge of Glass – 0% Window Frame – 26%	-43.8%
	X-Spacer	1.80	Centre of Glass – 61.8% Edge of Glass – 12.2% Window Frame – 26%	1.51	Centre of Glass – 67.6% Edge of Glass – 6.4% Window Frame – 26%	0.99	Centre of Glass – 74% Edge of Glass – 0% Window Frame – 26%	-44.9%
	T-Spacer	1.69	Centre of Glass – 63.3% Edge of Glass – 10.7% Window Frame – 26%	1.43	Centre of Glass – 68.1% Edge of Glass – 5.9% Window Frame – 26%	0.98	Centre of Glass – 74% Edge of Glass – 0% Window Frame – 26%	-41.7%
	% Variation	-6.1%		-5.2%		-0.8%		
Thermally Broken Aluminum Frame	H-Spacer	2.09	Centre of Glass – 58% Edge of Glass – 12.8% Window Frame – 29.3%	1.84	Centre of Glass – 61.6% Edge of Glass – 9.1% Window Frame – 29.3%	1.41	Centre of Glass – 70.7% Edge of Glass – 0% Window Frame – 29.3%	-32.3%
	X-Spacer	2.11	Centre of Glass – 60.3% Edge of Glass – 10.4% Window Frame – 29.3%	1.85	Centre of Glass – 63.6% Edge of Glass – 7.1% Window Frame – 29.3%	1.42	Centre of Glass – 70.7% Edge of Glass – 0% Window Frame – 29.3%	-32.7%
	T-Spacer	2.01	Centre of Glass – 62% Edge of Glass – 8.7% Window Frame – 29.3%	1.78	Centre of Glass – 65.5% Edge of Glass – 5.2% Window Frame – 29.3%	1.42	Centre of Glass – 70.7% Edge of Glass – 0% Window Frame – 29.3%	-29.7%
	% Variation	-4.4%		-4.1%		-0.3%		
Vinyl Frame	H-Spacer	1.65	Centre of Glass – 51.8% Edge of Glass – 20.2% Window Frame – 28%	1.42	Centre of Glass – 52% Edge of Glass – 20% Window Frame – 28%	0.93	Centre of Glass – 72% Edge of Glass – 0% Window Frame – 28%	-44.0%
	X-Spacer	1.68	Centre of Glass – 53.2% Edge of Glass – 18.7% Window Frame – 28%	1.43	Centre of Glass – 57% Edge of Glass – 15% Window Frame – 28%	0.92	Centre of Glass – 72% Edge of Glass – 0% Window Frame – 28%	-45.2%
	T-Spacer	1.57	Centre of Glass – 54.2% Edge of Glass – 17.8% Window Frame – 28%	1.34	Centre of Glass – 57.5% Edge of Glass – 14.5% Window Frame – 28%	0.92	Centre of Glass – 72% Edge of Glass – 0% Window Frame – 28%	-41.8%
	% Variation	-6.5%		-6.4%		-1.0%		

Table 11 - Summary of results (U-value, and glazing segment proportions)

Moving forward, the results obtained from the 36 simulations could be further analyzed in a hotbox apparatus. Prototypes of the window systems could be constructed and tested in a live simulation using the same boundary conditions to determine the accuracy of the results obtained from the 3D finite element heat transfer analysis. Results from a hotbox analysis could lead to further research on optimizing the best performing spacer system. Playing with the dimensions including the thickness of the ‘T’ intermediate and ‘U’ edge spacer could be performed to optimize the spacer system. Other composite plastic materials being used for warm edge spacers could be tested to determine a more optimal material of construction.

Another area of focus could be researching on constructability of the modelled window systems and investigate the impact on the performance of the window system. Constructability was not an area of focus for this research paper. It is assumed that all PVC spacer systems would be casted as a single assembly and inserted between the panes of glass, while metal spacer components would be formed individually and be bonded together with an epoxy. The constructability analysis could also consider exploring appropriate methods of handling and inserting the aerogel panes into the window systems and perhaps research an effective way to make an evacuated window system. Lastly, modelling the service life of a window system insulated with monolithic silica aerogel could help determine if it is economically viable.

At present monolithic silica aerogel is at an experimental and demonstrative phase showing promising qualities for application in glazing systems. Although many companies have developed structurally stable translucent aerogel blankets, further research must be done to improve the structural strength, without compromising the transparent qualities. Another potential research area could be to study and compare the properties of aerogel from different suppliers. Properties such as visible and solar energy transmissibility, thermal conductivity, light diffusion properties, and structural strength could be analyzed to determine an optimal monolithic silica aerogel material and supplier for glazing applications.

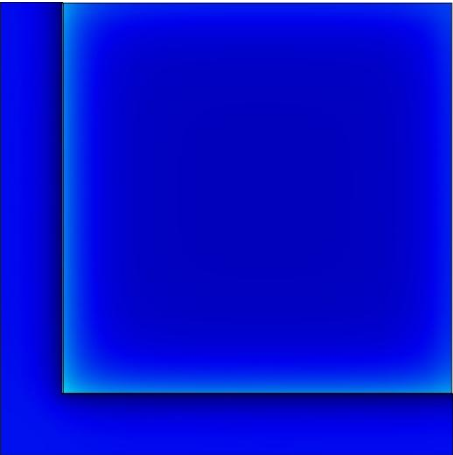
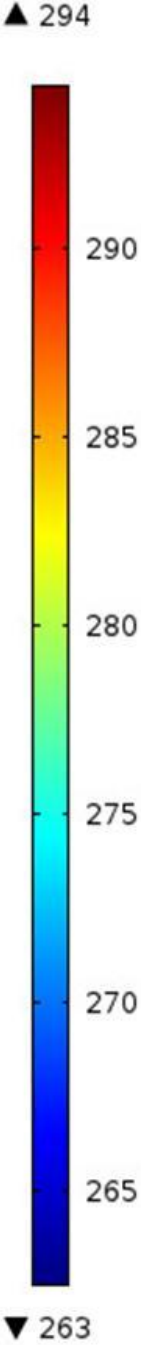
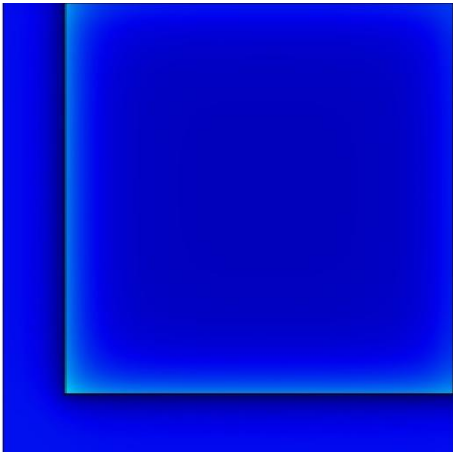
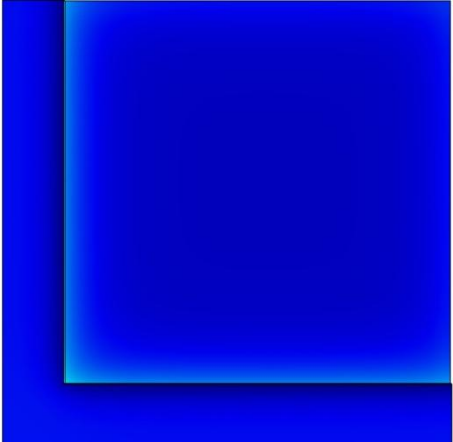
Appendix 1 – Thermographic Heat Transfer Diagrams

Solid Wood Framed Window Systems (Aluminum Spacers)		
	<p>UHWA6146_W_AL – Solid wood frame with ‘H’ intermediate and ‘U’ edge spacer constructed with aluminum.</p> <p>U-value = $1.87\text{W/m}^2\text{k}$ (32% improvement compared to 1D analysis)</p> <p>Centre of Glass – 62.1% Edge of Glass – 11.9% Window Frame – 26%</p>	
	<p>UXWA6146_W_AL – Solid wood frame with ‘X’ intermediate and ‘U’ edge spacer constructed with aluminum.</p> <p>U-value = $1.91\text{W/m}^2\text{k}$ (31% improvement compared to 1D analysis)</p> <p>Centre of Glass – 61.8% Edge of Glass – 12.2% Window Frame – 26%</p>	
	<p>UTWA6146_W_AL – Solid wood frame with ‘T’ intermediate and ‘U’ edge spacer constructed with aluminum.</p> <p>U-value = $1.80\text{W/m}^2\text{k}$ (34% improvement compared to 1D analysis)</p> <p>Centre of Glass – 65% Edge of Glass – 9% Window Frame – 26%</p>	

Solid Wood Framed Window Systems (Stainless Spacers)

	<p>UHWA6146_W_SS – Solid wood frame with ‘H’ intermediate and ‘U’ edge spacer constructed with stainless steel.</p> <p>U-value = 1.64W/m²k (24% improvement compared to 1D analysis)</p> <p>Centre of Glass – 64.7% Edge of Glass – 9.3% Window Frame – 26%</p>	
	<p>UXWA6146_W_SS – Solid wood frame with ‘X’ intermediate and ‘U’ edge spacer constructed with stainless steel.</p> <p>U-value = 1.65W/m²k (23% improvement compared to 1D analysis)</p> <p>Centre of Glass – 64.8% Edge of Glass – 9.2% Window Frame – 26%</p>	
	<p>UTWA6146_W_SS – Solid wood frame with ‘T’ intermediate and ‘U’ edge spacer constructed with stainless steel.</p> <p>U-value = 1.56W/m²k (22% improvement compared to 1D analysis)</p> <p>Centre of Glass – 65.7% Edge of Glass – 8.3% Window Frame – 26%</p>	

Solid Wood Framed Window Systems (Polyvinyl Chloride Spacers)

	<p>UHWA6146_W_PVC – Solid wood frame with ‘H’ intermediate and ‘U’ edge spacer constructed with PVC.</p> <p>U-value = 1.15W/m²k (4.4% improvement compared to 1D analysis)</p> <p>Centre of Glass – 74% Edge of Glass – 0% Window Frame – 26%</p>	
	<p>UXWA6146_W_PVC – Solid wood frame with ‘X’ intermediate and ‘U’ edge spacer constructed with PVC.</p> <p>U-value = 1.15W/m²k (3.8% improvement compared to 1D analysis)</p> <p>Centre of Glass – 74% Edge of Glass – 0% Window Frame – 26%</p>	
	<p>UTWA6146_W_PVC – Solid wood frame with ‘T’ intermediate and ‘U’ edge spacer constructed with PVC.</p> <p>U-value = 1.14W/m²k (4.3% improvement compared to 1D analysis)</p> <p>Centre of Glass – 74% Edge of Glass – 0% Window Frame – 26%</p>	

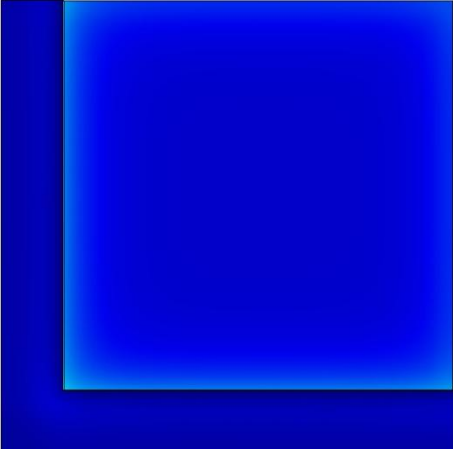
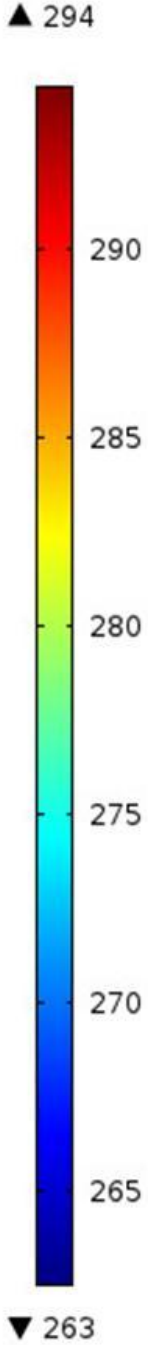
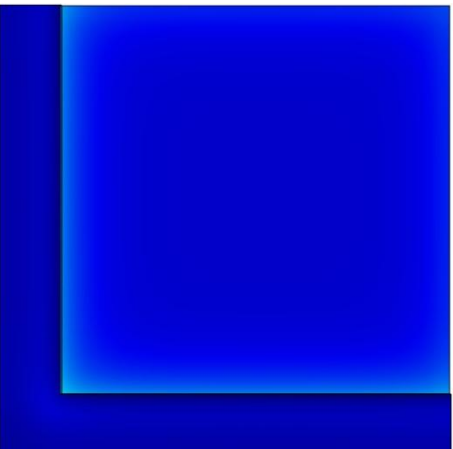
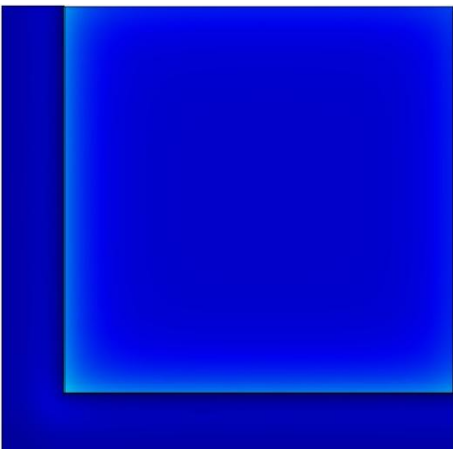
Thermally Broken Wooden Framed Window Systems (Aluminum Spacers)

	<p>UHWA6146_TBW_AL – Thermally broken wooden frame with ‘H’ intermediate and ‘U’ edge spacer constructed with aluminum.</p> <p>U-value = 1.77W/m²k (35% improvement compared to 1D analysis)</p> <p>Centre of Glass – 61% Edge of Glass – 13% Window Frame – 26%</p>	
	<p>UXWA6146_TBW_AL – Thermally broken wooden frame with ‘X’ intermediate and ‘U’ edge spacer constructed with aluminum.</p> <p>U-value = 1.80W/m²k (33% improvement compared to 1D analysis)</p> <p>Centre of Glass – 61.8% Edge of Glass – 12.2% Window Frame – 26%</p>	
	<p>UTWA6146_TBW_AL – Thermally broken wooden frame with ‘T’ intermediate and ‘U’ edge spacer constructed with aluminum.</p> <p>U-value = 1.69W/m²k (36.6% improvement compared to 1D analysis)</p> <p>Centre of Glass – 63.3% Edge of Glass – 10.7% Window Frame – 26%</p>	

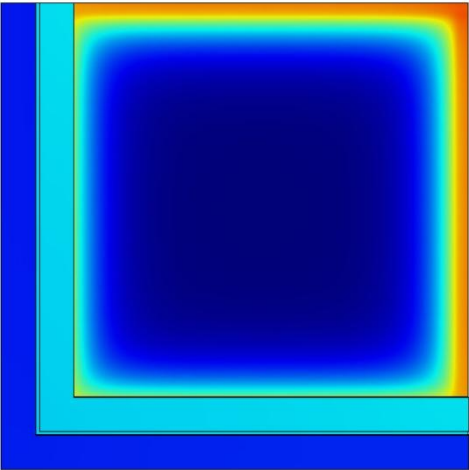
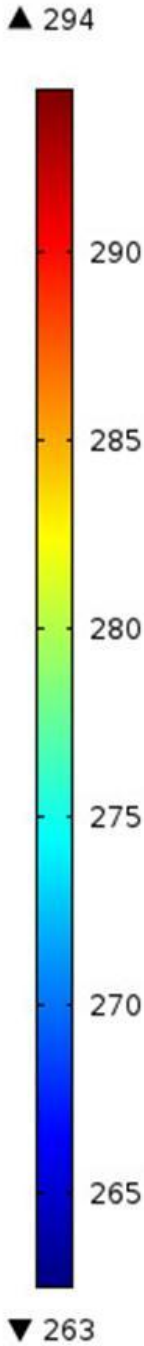
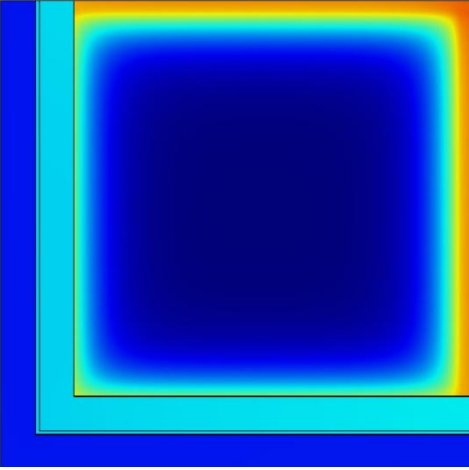
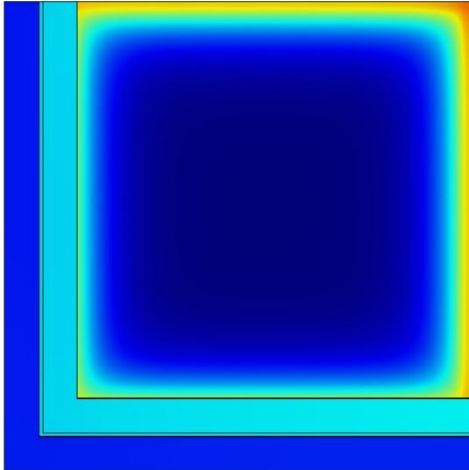
Thermally Broken Wooden Framed Window Systems (Stainless Steel Spacers)

	<p>UHWA6146_TBW_SS – Thermally broken wooden frame with ‘H’ intermediate and ‘U’ edge spacer constructed with stainless steel.</p> <p>U-value = 1.51W/m²k (27.8% improvement compared to 1D analysis)</p> <p>Centre of Glass – 64.1% Edge of Glass – 9.8% Window Frame – 26%</p>	
	<p>UXWA6146_TBW_SS – Thermally broken wooden frame with ‘X’ intermediate and ‘U’ edge spacer constructed with stainless steel.</p> <p>U-value = 1.51W/m²k (27.1% improvement compared to 1D analysis)</p> <p>Centre of Glass – 67.6% Edge of Glass – 6.4% Window Frame – 26%</p>	
	<p>UTWA6146_TBW_SS – Thermally broken wooden frame with ‘T’ intermediate and ‘U’ edge spacer constructed with stainless steel.</p> <p>U-value = 1.43W/m²k (25.9% improvement compared to 1D analysis)</p> <p>Centre of Glass – 68.1% Edge of Glass – 5.9% Window Frame – 26%</p>	

Thermally Broken Wooden Framed Window Systems (Polyvinyl Chloride Spacers)

	<p>UHWA6146_TBW_PVC – Thermally broken wooden frame with ‘H’ intermediate and ‘U’ edge spacer constructed with PVC.</p> <p>U-value = 0.99W/m²k (13% improvement compared to 1D analysis)</p> <p>Centre of Glass – 74% Edge of Glass – 0% Window Frame – 26%</p>	
	<p>UXWA6146_TBW_PVC – Thermally broken wooden frame with ‘X’ intermediate and ‘U’ edge spacer constructed with PVC.</p> <p>U-value = 0.99W/m²k (13.2% improvement compared to 1D analysis)</p> <p>Centre of Glass – 74% Edge of Glass – 0% Window Frame – 26%</p>	
	<p>UTWA6146_TBW_PVC – Thermally broken wooden frame with ‘T’ intermediate and ‘U’ edge spacer constructed with PVC.</p> <p>U-value = 0.98W/m²k (13% improvement compared to 1D analysis)</p> <p>Centre of Glass – 74% Edge of Glass – 0% Window Frame – 26%</p>	

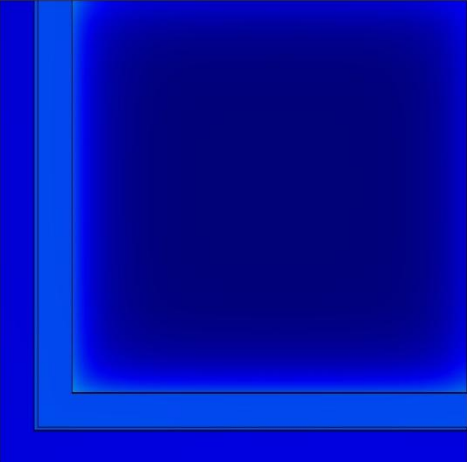
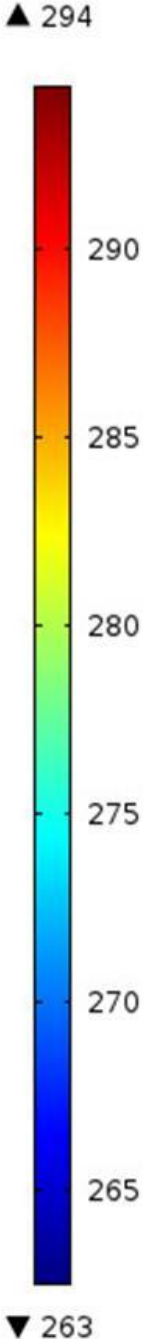
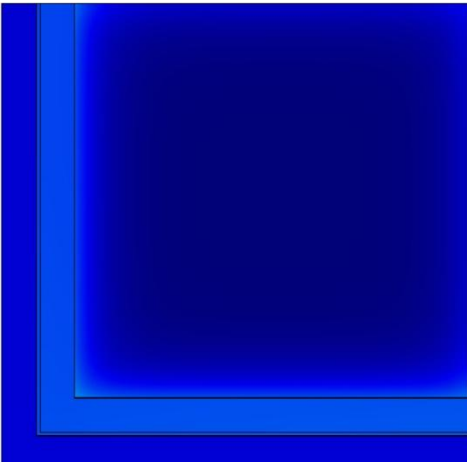
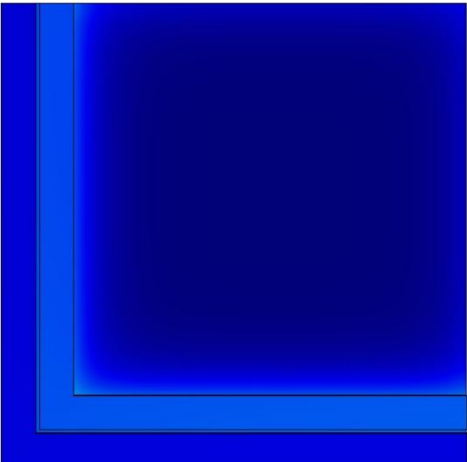
Thermally Broken Aluminum Framed Window Systems (Aluminum Spacers)

	<p>UHWA6146_TBAL_AL – Thermally broken aluminum frame with ‘H’ intermediate and ‘U’ edge spacer constructed with aluminum.</p> <p>U-value = 2.09W/m²k (95.9% improvement compared to 1D analysis)</p> <p>Centre of Glass – 58% Edge of Glass – 12.8% Window Frame – 29.3%</p>	
	<p>UXWA6146_TBAL_AL – Thermally broken aluminum frame with ‘X’ intermediate and ‘U’ edge spacer constructed with aluminum.</p> <p>U-value = 2.11W/m²k (95.8% improvement compared to 1D analysis)</p> <p>Centre of Glass – 60.3% Edge of Glass – 10.4% Window Frame – 29.3%</p>	
	<p>UTWA6146_TBAL_AL – Thermally broken aluminum frame with ‘T’ intermediate and ‘U’ edge spacer constructed with aluminum.</p> <p>U-value = 2.01W/m²k (96% improvement compared to 1D analysis)</p> <p>Centre of Glass – 62% Edge of Glass – 8.7% Window Frame – 29.3%</p>	

Thermally Broken Aluminum Framed Window Systems (Stainless Steel Spacers)

	<p>UHWA6146_TBAL_SS – Thermally broken aluminum frame with ‘H’ intermediate and ‘U’ edge spacer constructed with stainless steel.</p> <p>U-value = 1.84W/m²k (95% improvement compared to 1D analysis)</p> <p>Centre of Glass – 61.6% Edge of Glass – 9.1% Window Frame – 29.3%</p>	
	<p>UXWA6146_TBAL_SS – Thermally broken aluminum frame with ‘X’ intermediate and ‘U’ edge spacer constructed with stainless steel.</p> <p>U-value = 1.85W/m²k (96% improvement compared to 1D analysis)</p> <p>Centre of Glass – 63.6% Edge of Glass – 7.1% Window Frame – 29.3%</p>	
	<p>UTWA6146_TBAL_SS – Thermally broken aluminum frame with ‘T’ intermediate and ‘U’ edge spacer constructed with stainless steel.</p> <p>U-value = 1.78W/m²k (96% improvement compared to 1D analysis)</p> <p>Centre of Glass – 65.5% Edge of Glass – 5.2% Window Frame – 29.3%</p>	

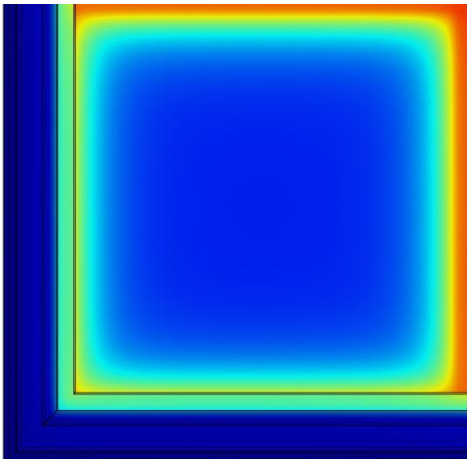
Thermally Broken Aluminum Framed Window Systems (Polyvinyl Chloride Spacers)

	<p>UHWA6146_TBAL_PVC – Thermally broken aluminum frame with ‘H’ intermediate and ‘U’ edge spacer constructed with PVC.</p> <p>U-value = 1.41W/m²k (97% improvement compared to 1D analysis)</p> <p>Centre of Glass – 70.7% Edge of Glass – 0% Window Frame – 29.3%</p>	
	<p>UXWA6146_TBAL_PVC – Thermally broken aluminum frame with ‘X’ intermediate and ‘U’ edge spacer constructed with PVC.</p> <p>U-value = 1.42W/m²k (97% improvement compared to 1D analysis)</p> <p>Centre of Glass – 70.7% Edge of Glass – 0% Window Frame – 29.3%</p>	
	<p>UTWA6146_TBAL_PVC – Thermally broken aluminum frame with ‘T’ intermediate and ‘U’ edge spacer constructed with PVC.</p> <p>U-value = 1.42W/m²k (97% improvement compared to 1D analysis)</p> <p>Centre of Glass – 70.7% Edge of Glass – 0% Window Frame – 29.3%</p>	

Vinyl Framed Window Systems (Aluminum Spacers)

	<p>UHWA6146_Vinyl_AL – Vinyl frame with ‘H’ intermediate and ‘U’ edge spacer constructed with aluminum.</p> <p>U-value = 1.65W/m²k (38.1% improvement compared to 1D analysis)</p> <p>Centre of Glass – 51.8% Edge of Glass – 20.2% Window Frame – 28%</p>	
	<p>UHWA6146_Vinyl_AL – Vinyl frame with ‘X’ intermediate and ‘U’ edge spacer constructed with aluminum.</p> <p>U-value = 1.68W/m²k (37% improvement compared to 1D analysis)</p> <p>Centre of Glass – 53.2% Edge of Glass – 18.7% Window Frame – 28%</p>	
	<p>UHWA6146_Vinyl_AL – Vinyl frame with ‘T’ intermediate and ‘U’ edge spacer constructed with aluminum.</p> <p>U-value = 1.57W/m²k (40% improvement compared to 1D analysis)</p> <p>Centre of Glass – 54.2% Edge of Glass – 17.8% Window Frame – 28%</p>	

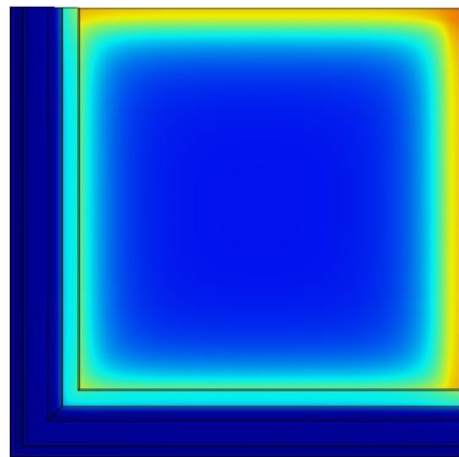
Vinyl Framed Window Systems (Stainless Steel Spacers)



UHWA6146_Vinyl_SS – Vinyl frame with 'H' intermediate and 'U' edge spacer constructed with stainless steel.

U-value = 1.42W/m²k (31.3% improvement compared to 1D analysis)

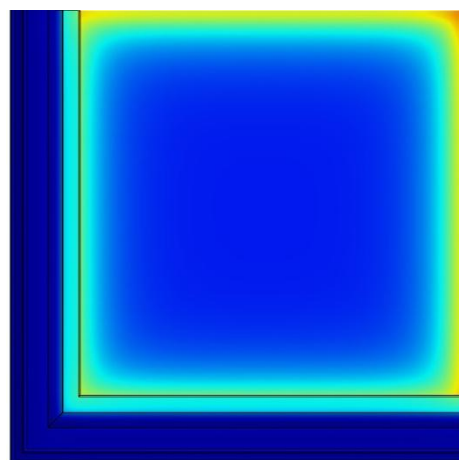
Centre of Glass – 52%
Edge of Glass – 20%
Window Frame – 28%



UHWA6146_Vinyl_SS – Vinyl frame with 'X' intermediate and 'U' edge spacer constructed with stainless steel.

U-value = 1.43W/m²k (30.1% improvement compared to 1D analysis)

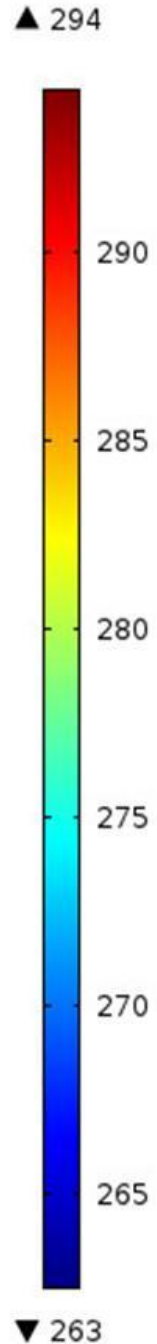
Centre of Glass – 57%
Edge of Glass – 15%
Window Frame – 28%



UHWA6146_Vinyl_SS – Vinyl frame with 'T' intermediate and 'U' edge spacer constructed with stainless steel.

U-value = 1.34W/m²k (29.8% improvement compared to 1D analysis)

Centre of Glass – 57.5%
Edge of Glass – 14.5%
Window Frame – 28%



Vinyl Framed Window Systems (Polyvinyl Chloride Spacers)

	<p>UHWA6146_Vinyl_PVC – Vinyl frame with ‘H’ intermediate and ‘U’ edge spacer constructed with PVC.</p> <p>U-value = 0.93W/m²k (19.1% improvement compared to 1D analysis)</p> <p>Centre of Glass – 72% Edge of Glass – 0% Window Frame – 28%</p>	<p>▲ 294</p> <p>290</p> <p>285</p> <p>280</p> <p>275</p> <p>270</p> <p>265</p> <p>▼ 263</p>
	<p>UHWA6146_Vinyl_PVC – Vinyl frame with ‘X’ intermediate and ‘U’ edge spacer constructed with PVC.</p> <p>U-value = 0.92W/m²k (19.8% improvement compared to 1D analysis)</p> <p>Centre of Glass – 72% Edge of Glass – 0% Window Frame – 28%</p>	
	<p>UHWA6146_Vinyl_PVC – Vinyl frame with ‘T’ intermediate and ‘U’ edge spacer constructed with PVC.</p> <p>U-value = 0.92W/m²k (19.6% improvement compared to 1D analysis)</p> <p>Centre of Glass – 72% Edge of Glass – 0% Window Frame – 28%</p>	

Appendix 2 – Photographs of Prototype



'U' Edge and 'H' Intermediate Spacer (Framed)



'U' Edge and 'H' Intermediate Spacer



'U' Edge and 'X' Intermediate Spacer (Framed)



'U' Edge and 'X' Intermediate Spacer



'U' Edge and 'T' Intermediate Spacer (Framed)



'U' Edge and 'T' Intermediate Spacer

References

- [1] Active Space Technologies. (2013). Aerogels – The Future of Thermal Insulation for Space Applications. Retrieved from <http://esther.ist.utl.pt/pages/yurisnight2011/ActiveSpaceTech.pdf>
- [2] Asdrubali, F., Baldinelli, G., Bianchi, F. (2013). Influence of Cavities Geometric and Emissivity on the Overall Thermal Performance of Aluminum Frames for Windows. *Energy and Buildings*, 60, 298-309.
- [3] Aspen Aerogel. (2014). About Aerogel. Retrieved from <http://www.aerogel.com/resources/about-aerogel/>
- [4] Baetens, R., Jelle, B. P., & Gustavsen, A. (2010). Aerogel Insulation for Building Applications: A state-of-the-art Review. *Energy and Buildings*, 43(4), 761-769.
- [5] Berardi, U. (2015) The Development of Monolithic Aerogel Glazed Window for Energy Retrofitting Project. *Applied Energy*, 154, 603-615.
- [6] Buratti, C., & Moretti, E. (2011). Lighting and Energetic Characteristics of Transparent Insulating Materials: Experimental Data and Calculation. *Indoor and Built Environment*, 20(4), 400-411.
- [7] Burrati, C., & Moretti, M. (2012). Experimental Performance Evaluation of Aerogel Glazing Systems. *Applied Energy*, 97, 430-437.
- [8] Duer, K., & Svendsen, S. (1998). Monolithic Silica Aerogel in Superinsulating Glazings. *Solar Energy*, 63(4), 259 - 267.
- [9] Fricke, J. (1992). Aerogels and their Applications. *Journal of Non-Crystalline Solids*, 147-148, 356-362.
- [10] Fricke, J., Caps, R., Butner, D., Heinemann, U., & Hummer, E. (1987). Silica Aerogel - A Light Transmitting Thermal Superinsulator. *Journal of Non-Crystalline Solids*, 95 & 96, 1167 - 1174.
- [11] Gustavsen, A., Grynning, S., Arasteh, D., Jelle, B., Goudey, H. (2011). Key Elements of and Material Performance Targets for Highly Insulating Window Frames. *Energy and Buildings*, 43, 2583 - 2595.
- [12] Hrubesh, L. W. (1998). Aerogel Applications. *Journal of Non-Crystalline Solids*, 225, 335 - 342.
- [13] Hutcheon, N. B., & Handegord, G. O. P. (1995). *Building Science for a Cold Climate*. Canada: National Research Council Canada
- [14] Incropera, F. P., & DeWitt, D. P. (2002). *Introduction to Heat Transfer*. New York, NY: John Wiley & Sons Inc.
- [15] Jelle, B. P., Hynd, A., Gustavsen, A., Arasteh, D., Goudey, H., & Hart, R. (2011). Fenestration of today and tomorrow: A State-of-the-art Review and Future Research Opportunities. *Solar Energy Materials and Solar Cells*, 96, 1 - 28.
- [16] Jensen, K. I., Schultz, K. M., & Kristiansen, F. H. (2004). Development of Windows Based on Highly Insulating Aerogel Glazings. *Journal of Non-Crystalline Solids*, 350, 351-357
- [17] Muslum, A., Hasan, K., Mirac, K. (2014). Flo and Heat Transfer in Double, Triple, and Quadruple Pane Windows. *Energy and Buildings*, 86, 394 - 402.

- [18] Rubin, M., & Lampert, C. M. (1982). Transparent Silica Aerogels for Window Insulation. *Solar Energy Materials*, 7, 393-400.
- [19] Schultz, J. M., & Jensen, K. I. (2008). Evacuated Aerogel Glazings. *Vacuum*, 82(7), 723-729.
- [20] Schultz, J. M., Jensen, K. I., & Kristiansen, F. H. (2005). Super Insulating Aerogel Glazing. *Solar Energy Materials and Solar Cells*, (89), 275 - 285.
- [21] Shukla, N., Fallahi, A., & Kosney, J. (2014). Aerogel thermal Insulation—Technology Review and Cost Study for Building Enclosure Applications. *ASHRAE Transactions*, 120, 294-307.
- [22] Sujoy, P., Biswanath, R., Subhasis, N. (2009). Heat Transfer Modelling on Windows and Glazing under exposure of Solar Radiation. *Energy and Buildings*, 41, 654-661.
- [23] Takeshi, I., Tao, G., Steiner, G., Jelle, B., Gustavsen, A. (2014). Aerogel Granulate Glazing Facade and their Application Potential from Energy Saving Perspective. *Applied Energy*, 142, 179 - 191.
- [24] Wang, T. (2014). Energy Retrofit of Kaven Hall with Aerogel Application. Worcester Polytechnic Institute, Retrieved from: https://www.wpi.edu/Pubs/E-project/Available/E-project-032714-112207/unrestricted/MQP_Taoning_Wang.pdf
- [25] Van Den Bergh, S., Hart, R., Jelle, B., Gustavsen, A. (2012). Window Spacers and Edge Seals in Insulated
- [26] Glazing Units: A State of the Art Review and Future Perspectives. *Energy and Buildings*, 58, 263-280.
- [27] Van Den Bossche, N., Buffel, L., Janssens, A. (2015). Thermal Optimization of Window Frames. *Science Direct*. 00, 000-000. 6th International Building Physics Conference.